Bergische Universität Wuppertal
Fachbereich C - Mathematik und
Naturwissenschaften
Fachgruppe Physik

Quasiparticles, Dynamics and Thermodynamics in the XX Chain

Dissertation
zur Erlangung der Doktorwürde
des Fachbereiches C (Fachgruppe Physik)
der Bergischen Universität Wuppertal

vorgelegt
am 7. Januar 2008
von Klaus Wiele
aus Wuppertal

WUB-DIS 2008-01
Januar 2008

Die Dissertation kann wie folgt zitiert werden:

urn:nbn:de:hbz:468-20080112
[http://nbn-resolving.de/urn/resolver.pl?urn=urn%3Anbn%3Ade%3Ahbz%3A468-20080112]

Contents

List of Figures

1 Introduction

The physical phenomenon of magnetism has been known for a long time. The eldest written text about the *lodestone* dates maybe back to the ancient Greek philosopher Thales of Miletus [1] in the sixth century BC. Nearly two thousand years later the use of a compass has been reported by medieval monks in the thirteenth century and some two hundred years earlier in China. But the fundamental origins of magnetism could not be understood without quantum mechanics.

This theory was given birth in 1900 when Max Planck [2] used the ad hoc hypothesis of quantized energy to explain the black body radiation. Then it was further promoted by Albert Einstein [3] who used the photon to explain the photoelectric effect in 1905 and Nils Bohr [4] who calculated the spectral lines of the hydrogen atom in 1914. The famous experiment by Otto Stern and Walther Gerlach [5] in 1922 gave evidence of a half-integer intrinsic angular momentum of the electron, which is nowadays known as its *spin*. A theoretical explanation of spins was published by Samuel Goudsmit and George Uhlenbeck [6] in 1925 and formalized a year later by Wolgang Pauli who introduced the Pauli spin matrices. A consistent formulation of quantum mechanics was given independently by Erwin Schrödinger [7] (*wave mechanics*) and Werner Heisenberg [8, 9] (*matrix mechanics*) around 1926. The theory successfully describes all atomic spectra.

In 1928 Werner Heisenberg [10] formulated an atomic model for ferromagnetism based on spin interaction. Since then the complete solution of the original three-dimensional *Heisenberg model* has eluded the theoretical physicists. But in 1931 Hans Bethe [11] succeeded in solving the model in at least one dimension by a method later called *Bethe ansatz*. He found a way to diagonalize the Hamiltonian analytically. Thus he derived a set of coupled transcendental equations whose solutions uniquely determine the spectrum (eigenvalues) and wave functions (eigenvectors) of the Hamiltonian. In modern notation these equations are the Bethe ansatz equations (2.22).

Since then the field of one-dimensional solid state physics has flourished. Nowadays a whole family of related models is under scrutiny with different couplings in spin space. The original model included nearest-neighbor interaction only but long-range versions have been studied as well. Many of them share the feature of analytical solvability (*integrability*). Thus they provide a quantum mechanical paradigm for collective phenomena.

This work is part of these one-dimensional studies. We investigate the anisotropic Heisenberg model (XXZ model) with uniform nearest-neighbor interaction at the critical point $\Delta = 0$ (XX model) and the isotropic Heisenberg model with inverse-square interaction (Haldane-Shastry model) which was introduced independently by Duncan Haldane [12] and Sriram Shastry [13] in 1988.

In Sec. 2 we will precisely define the XXZ model and briefly describe its solution, i.e., calculate the energy eigenvalues and eigenstates of the Hamiltonian. We do this in a generalization of Bethe's original approach (coordinate Bethe ansatz) in Sec. 2.2, following Jacques des Cloizeaux and Michael Gaudin [14]. The next subsection (Sec. 2.3) reviews this solution from a much broader algebraic point of view where the Bethe ansatz equations emerge as a concistency condition of the underlying Yang-Baxter algebra. This *algebraic Bethe ansatz* arose around 1979 in Leningrad [15] and is used in Sec. 2.4 to derive exact expressions for certain dynamic spin structure factors. They were given by the Lyon group in 1999 [16] and have been specialized to the XX model by Karbach et. al. [17, 18].

Sec. 3 is devoted to the XX model. It consists of subsections about magnons (Sec. 3.1), fermions (Sec. 3.2), spinons (Sec. 3.3), and dynamic spin structure factors (Sec. 3.4). In Sec. 3.2.1 we refer the momentum pattern of fermions which uniquely identifies every excitation. Then we formulate the thermodynamics of the XX model in terms of fermions in Sec. 3.2.2. The result will be compared in Sec. 3.3.5 to the spinonic result. The subsection about spinons is worked out in greater detail because there we report formerly unknown properties. For the first time the spinon interaction is extracted (Sec. 3.3.2), and a spinonic Bethe ansatz is proposed (Sec. 3.3.3). Then we present spinon orbital interaction (Sec. 3.3.4) and a spinonic formulation of thermodynamics (Sec. 3.3.5). In Sec. 3.4 new exact formulas for the dynamic spin structure factor $S_{-+}(q,\omega)_0$ are presented thus opening finite

systems with up to several thousand sites for the numerical analysis. Also these formulas are expanded analytically for the infinite system. We investigate the excitations of classes with up to four spinons for even and odd chain length at zero temperature.
Sec. 4 is about the Haldane-Shastry model which has inverse-square interaction. Following the original work from Haldane [12] we introduce spinons and establish a Bethe ansatz formalism analogously to the XX study in Sec. 3.3.3. Then we derive the interaction energy of spinonic orbitals in Sec. 4.3 and formulate the thermodynamics in terms of spinons in Sec. 4.4.
Some technical details are swapped into the appendices A-E. In part F a short introduction into the theory of neutron optics can be found. There the dynamic spin structure factors of Secs. 2.4 and 3.4 are related to the experimental setup. We explain how information about the inner structure of matter can be experimentally extracted that is encoded in dynamic spin structure factors.

Related Publications

The main results of this work have been published in the following articles:

- M. Arikawa, M. Karbach, G. Müller, and K. Wiele. Spinon excitations in the XX chain: spectra, transition rates, observability. *J. Phys. A: Math. Gen.* **39**, 10623 (2006).
- M. Karbach, G. Müller, and K. Wiele. Interaction and thermodynamics of spinons in the XX chain. *cond-mat/07103097* (2007).

They continue the work of my diploma thesis which has been published in

- D. Biegel, M. Karbach, G. Müller, and K. Wiele. Spectrum and transition rates of the XX chain analyzed via Bethe ansatz. *Phys. Rev. B* **69**, 174404 (2004).

2 The XXZ model

2.1 Hamiltonian and Basic Properties

In 1928 Heisenberg [10] wrote down a microscopic quantum mechanical model for ferromagnetism. This model was three-dimensional with the intention to explain the ferromagnetism of iron, cobalt and nickel which are of cubic face-centered and cubic body-centered atomic structure. The spectrum of the model was given in 1931 by Bethe [11] for the by far simpler case of one dimension. In the notation of today the Hamiltonian of the linear chain of N atoms reads

$$\mathcal{H}_{\mathrm{XXX}} = J \sum_{i=1}^{N} \vec{S}_i \cdot \vec{S}_{i+1}, \qquad \vec{S}_{N+1} = \vec{S}_1, \tag{2.1}$$

where the vector $\vec{S}_i$ denotes the spin operator at the lattice position i. The model describes the interaction of N spins one-half at sites i along a chain with periodically closed boundary conditions ($S_{N+1} = S_1$). The idea of closing the chain to a circle appears rather artifically and should be regarded as a mathematical simplification. The periodic closing reduces boundary effects and thus approximates the experimental situation where chains of at least several hundered sites are common. It also simplifies the mathematical treatment of the model. In the present work we aim numerically at large systems (several thousand sites) and analytically at the limit of the infinite system. In both cases the special choice of boundary conditions apparently leads to vanishing finite-size corrections only.

The interaction of the spins in (2.1) is restricted to nearest neighbors and uniform throughout the chain. This assumption goes back to Heitler and London [19, 20] who found that the exchange coupling of uncharged atoms decreases exponentially as a function of their distance. The interaction is ferromagnetic for $J < 0$ and antiferromagnetic for $J > 0$.

Heisenberg considered spins one-half because the magnetism of the ferroelectrica originates from single valence electrons. The same is true for many one-dimensional realizations of the Heisenberg model. In this case the components of the spin vectors are the three two-dimensional Pauli matrices σ^μ,

$$\vec{S}_i = (S_i^x, S_i^y, S_i^z), \qquad S_i^\mu = \frac{\hbar}{2}\sigma_i^\mu, \qquad \mu = x, y, z. \tag{2.2}$$

We will use units such that $\hbar$ becomes unity everywhere except in App. F which relates to the experiment. The index i indicates the lattice site the operator acts on. As a basis in spin space we choose the up-spin and down-spin vectors

$$|\uparrow\rangle = \begin{pmatrix} 1 \\ 0 \end{pmatrix}, \qquad |\downarrow\rangle = \begin{pmatrix} 0 \\ 1 \end{pmatrix}. \tag{2.3}$$

In this basis the matrix representation of the Pauli matrices is given by

$$\sigma^x = \begin{pmatrix} 0 & 1 \\ 1 & 0 \end{pmatrix}, \qquad \sigma^y = \begin{pmatrix} 0 & -\mathrm{i} \\ \mathrm{i} & 0 \end{pmatrix}, \qquad \sigma^z = \begin{pmatrix} 1 & 0 \\ 0 & -1 \end{pmatrix}. \tag{2.4}$$

The Hamiltonian (2.1) therefore operates on a Hilbert space of dimension 2^N. It is nowadays called the *isotropic (anti)ferromagnetic Heisenberg chain* the attribute "isotropic" relating to the uniform coupling in spin space. A natural generalization to anisotropic spin coupling is the so-called XXZ model

$$\mathcal{H}_{\mathrm{XXZ}} = J \sum_{i=1}^{N} \left[S_i^x S_{i+1}^x + S_i^y S_{i+1}^y + \Delta S_i^z S_{i+1}^z \right] \tag{2.5}$$

with the anisotropy parameter Δ. Again periodic boundary conditions are assumed. According to the numerical value of the anisotropy we distinguish the axial regime $|\Delta| > 1$, the planar regime $|\Delta| < 1$, the isotropic point $|\Delta| = 1$ (XXX model) and the critical point $\Delta = 0$ (XX model).
These names are derived from certain properties of the corresponding classical model, where the spin operators S_i^μ are replaced by ordinary vectors of length 1/2 (see [14]). In the classical model the ground state for $\Delta > 1$ is the state where all spin vectors are parallel to the quantization (z) axis but with alternating directions. For $\Delta < -1$ all spins are parallel to the z-axis and point in the same directions. But in the regime $|\Delta| < 1$ the spin vectors lie within the xy plane. The isotropic point $\Delta = 1$ of course referes to the identical coupling for all three directions in spin space.
It is useful to introduce the creation and annihilation operators

$$S_i^+ = S_i^x + \mathrm{i}S_i^y = \begin{pmatrix} 0 & 1 \\ 0 & 0 \end{pmatrix}, \qquad S_i^- = S_i^x - \mathrm{i}S_i^y = \begin{pmatrix} 0 & 0 \\ 1 & 0 \end{pmatrix}. \tag{2.6}$$

In these operators the Hamiltonian (2.5) reads

$$\mathcal{H}_{\mathrm{XXZ}} = J \sum_{i=1}^{N} \Big[\frac{1}{2} \left(S_i^+ S_{i+1}^- + S_i^- S_{i+1}^+ \right) + \Delta S_i^z S_{i+1}^z \Big]. \tag{2.7}$$

This notation immediately shows the Hamilton operator to conserve the number of inverted spins. It is also elementary to prove that the component

$$S_T^z = \sum_{i=1}^{N} S_i^z \tag{2.8}$$

of the total spin along the quantization axis (z) is a conserved quantity, $[\mathcal{H}_{\mathrm{XXZ}}, S_T^z] = 0$. The following subsection will use that the Hamilton operator (2.7) commutes with the translation operator which shifts every spin by one site. It is therefore possible to construct a translational invariant basis.

2.2 Solution 1: Coordinate Bethe Ansatz

The isotropic one-dimensional Heisenberg model was solved by Bethe [11] in 1931. He made an ingenious parameter-dependend ansatz for the eigenvectors. His trial wave functions are eigenfunctions as long as the parameters solve a specific set of transcendental equations which are now called Bethe ansatz equations. Thus the calculation of the energies and eigenfunctions of the Hamiltonian is reduced to the solution of a set of coupled nonlinear equations. The method was generalized by des Cloizeaux and Gaudin [14] in 1966 to the case of the anisotropic XXZ model. In the following we will briefly outline their calculation.
First, we remember that the z-component of the total spin is a conserved quantity. We name the corresponding quantum number m and write it as

$$m = \frac{N}{2} - r. \tag{2.9}$$

Thus $0 \leq r \leq N$ denotes the number of down-spins. Since the Hamilton operator does not change the number of up- and down-spins it is possible to find a basis of translationally invariant eigenvectors for every sector of r down-spins. In this basis $\mathcal{H}_{\mathrm{XXZ}}$ decomposes into $N+1$ blocks with dimensions $\binom{N}{r}$.
Let

$$|F\rangle = |\uparrow \cdots \uparrow\rangle \tag{2.10}$$

denote the state where all spins are aligned and pointing upward[1]. It is the ground state of the ferromagnet and its energy is $E_F = \Delta/4$. Every other eigenstate of (2.7) can be obtained from $|F\rangle$ by applying local spin flip operators S_i^- (2.6), where

$$S_i^-|\cdots\uparrow\cdots\rangle = |\cdots\downarrow\cdots\rangle \qquad \text{and} \qquad S_i^-|\cdots\downarrow\cdots\rangle = 0. \tag{2.11}$$

Hence all eigenstates of $\mathcal{H}_{\mathrm{XXZ}}$ are of the form

$$|\psi(n_1, n_2, \ldots, n_r)\rangle = \sum_{n_1<\cdots<n_r} a(n_1, \ldots, n_r) S_{n_1}^- \cdots S_{n_r}^- |F\rangle \tag{2.12}$$

where again r is the number of down-spins. The eigenvalue equation imposes conditions for the yet undetermined coefficients $a(n_1, \ldots, n_r)$. We define the reduced energy

$$\epsilon = \frac{E - E_F}{N} \tag{2.13}$$

where E is the energy of the state (2.12). The eigenvalue equation for (2.12) then leads to the consistency equations

$$2N\epsilon\, a(n_1, \ldots, n_r) = J \sum \left[a(n_1', \ldots, n_r') - \Delta a(n_1, \ldots, n_r)\right] \tag{2.14}$$

with $1 \le n_1 < \cdots < n_r \le N$ and where the coefficient $a(n_1', \ldots, n_r')$ is obtained from $a(n_1, \ldots, n_r)$ by changing one number n_i by one unit. The sum is over all possible coefficients $a(n_1', \ldots, a_r')$. Bethe's celebrated idea is the ansatz

$$a(n_1, \ldots, n_r) = \sum_{\mathcal{P}} \exp\left(\mathrm{i}\sum_{j=1}^{r} k_{\mathcal{P}j} n_j + \frac{\mathrm{i}}{2}\sum_{i<j} \theta_{\mathcal{P}i\mathcal{P}j}\right) \tag{2.15}$$

where the sum over $\mathcal{P}$ is over all $r!$ permutations of the labels $\{1, \ldots, r\}$ and $\mathcal{P}i$ is the label by which i is replaced under the permutation $\mathcal{P}$. The wave numbers k_i and phase angles θ_{ij} are yet undetermined. By (2.15) the coefficients are defined for the wider range $0 \le n_1 \le \cdots \le n_r \le N$ of the parameters and satisfy the equations

$$\begin{aligned} & 2N\epsilon a(n_1, \ldots, n_r) \qquad (2.16)\\ = \; & J\sum_{i=1}^{N}\left[a(n_1, \ldots, n_i+1, \ldots, n_r) + a(n_1, \ldots, n_i-1, \ldots, n_r) - 2\Delta a(n_1, \ldots, n_i, \ldots, n_r)\right] \end{aligned}$$

which reduce to the eigenvalue equations (2.14) if the conditions

$$a(\cdots, n_i+1, n_i+1, \cdots) + a(\cdots, n_i, n_i, \cdots) = 2\Delta a(\cdots, n_i, n_i+1, \cdots) \tag{2.17}$$

are fulfilled and thus the unwanted terms cancel. These conditions translate into the equations

$$-\cot(\tfrac{1}{2}\theta_{ij}) = \Delta\left[\frac{\cot(\frac{1}{2}k_i) - \cot(\frac{1}{2}k_j)}{(1-\Delta)\cot(\frac{1}{2}k_i)\cot(\frac{1}{2}k_j) - (1+\Delta)}\right] \tag{2.18}$$

relating the phase angles θ_{ij} to the momenta k_i. The periodic boundary conditions imply

$$a(n_1, n_2, \ldots, n_r) = a(n_2, \ldots, n_r, n_1 + N) \tag{2.19}$$

[1] It is common usage to refer to the positive z-axis as the upward direction

and hence

$$Nk_i = 2\pi\lambda_i + \sum_{j=1}^{N} \theta_{ij}, \qquad i = 1, \ldots, r \tag{2.20}$$

where the Bethe quantum numbers λ_i are integers. Every state is completely determined by the corresponding set of Bethe quantum numbers. The total energy and wave number are given by

$$E = \sum_{i=1}^{r} (\cos k_i - \Delta), \qquad k = \sum_{i=1}^{r} k_i = \frac{2\pi}{N} \sum_{i=1}^{r} \lambda_i \tag{2.21}$$

and the magnon momenta k_i are the solutions of the *Bethe ansatz equations* [14]

$$\mathrm{e}^{\mathrm{i}Nk_i} = \prod_{j \neq i}^{r} \Big[- \frac{1 + \mathrm{e}^{\mathrm{i}(k_i + k_j)} - 2\Delta \mathrm{e}^{\mathrm{i}k_i}}{1 + \mathrm{e}^{\mathrm{i}(k_i + k_j)} - 2\Delta \mathrm{e}^{\mathrm{i}k_j}} \Big], \qquad i = 1, \ldots, r. \tag{2.22}$$

The formulas (2.21) and (2.22) are given in the notation of [18]. There these equation were rewritten in terms of the anisotropy parameter

$$\gamma = \arccos \Delta \qquad (0 \leq \gamma \leq \pi/2) \tag{2.23}$$

and the rapidities

$$y_i = \tan \frac{\gamma}{2} \cot \frac{k_i}{2}, \qquad i = 1, \ldots, r \tag{2.24}$$

which stay real even if the k_i become complex. In these variables the equations (2.22) read

$$\Big(\frac{c_2 y_i + \mathrm{i}}{c_2 y_i - \mathrm{i}} \Big)^N = \prod_{j \neq i}^{r} \frac{c_1(y_i - y_j) + \mathrm{i}(1 - y_i y_j)}{c_1(y_i - y_j) - \mathrm{i}(1 - y_i y_j)} \tag{2.25}$$

with $c_1 = \cot \gamma$ and $c_2 = \cot(\gamma/2)$. Taking the logarithm yields the *trigonometric Bethe ansatz equations*

$$N\phi(c_2 y_i) = 2\pi I_i + \sum_{j \neq i}^{r} \phi\Big(c_1 \frac{y_i - y_j}{1 - y_i y_j} \Big), \qquad i = 1, \ldots, r \tag{2.26}$$

with $\phi(x) = 2 \arctan(x)$. Every solution is characterized by a set of integer or half integer Bethe quantum numbers I_i which distinguish between the different branches of the logarithm. The energy and wave number (2.21) then transform into

$$E = \frac{2}{c_2 + c_2^{-1}} \sum_{i=1}^{r} \frac{y_i - y_i^{-1}}{c_2 y_i + (c_2 y_i)^{-1}}, \qquad k = \pi r - \frac{2\pi}{N} \sum_{i=1}^{r} I_i. \tag{2.27}$$

2.3 Solution 2: Algebraic Bethe Ansatz

The algebraic Bethe ansatz or *Quantum Inverse Scattering Method* provides the mathematical background for solving many integrable quantum spin models. It has been introduced by the Leningrad school around 1979. Special articles on the XXX and XXZ model are written by Faddeev and Takhtadzhan [21] and Kulish and Sklyanin [22]. Detailed explanations are found in a summer school article by Faddeev [23]. An account of broader scope is given in the textbooks [24, 25].

The basic idea is to construct a set of infinitely many operators which commute with the Hamiltonian. Since each commuting operator is related to a conservation law this procedure generates infinitely many conserved quantites and thus proves the Hamiltonian to be integrable. During this procedure the Bethe ansatz equations (2.25) naturally appear as a necessary condition for the method to work. The algebraic Bethe ansatz involves two different vector spaces, (i) the Hilbert space of physical states and (ii) the so-called auxiliary space. The Hilbert space is a product space of dimension 2^N,

$$\mathcal{H}_N = \bigotimes_{n=1}^{N} \eta_n, \qquad \eta_n = \mathbb{C}^2 \tag{2.28}$$

and the auxiliary space is $\mathbb{C}^2$. The creation and annihilation operators on $\mathcal{H}_N$ are defined by

$$\sigma_n^{\pm} = \underset{1}{\mathbb{I}} \otimes \cdots \otimes \underset{n-1}{\mathbb{I}} \otimes (\underset{n}{\sigma^x} \pm \mathrm{i}\sigma^y) \otimes \underset{n+1}{\mathbb{I}} \otimes \cdots \otimes \underset{N}{\mathbb{I}} \tag{2.29}$$

and act on η_n. They are, of course, the same as (2.6) save for an obvious factor of two. But here we emphasize the action on the tensor product structure of the Hilbert space. The symbol $\mathbb{I}$ denotes the identity operator on $\mathbb{C}^2$. On the auxiliary space a local transition matrix, the so-called *Lax operator*, is defined by

$$L_n(\lambda) = \begin{pmatrix} \lambda\mathbb{I}_n + (\mathrm{i}/2)\sigma_n^z & (\mathrm{i}/2)\sigma_n^- \\ (\mathrm{i}/2)\sigma_n^+ & \lambda\mathbb{I}_n - (\mathrm{i}/2)\sigma_n^z \end{pmatrix} = \lambda\mathbb{I}_a \otimes \mathbb{I}_n + \frac{\mathrm{i}}{2} \sum_{\alpha=x,y,z} \sigma_a^\alpha \otimes \sigma_n^\alpha, \qquad \lambda \in \mathbb{C} \tag{2.30}$$

where the elements are operators on the Hilbert space $\mathcal{H}_N$ and act non-trivially on η_n only. In the tensor product form the identity $\mathbb{I}_a$ and the Pauli matrices σ_a^α act on the auxiliary space (index a) and the identity and the Pauli matrices on the right act on η_n (index n). Thus the Lax operator is a two-by-two matrix on the auxiliary space whose elements are operators acting on the Hilbert space $\mathcal{H}_N$. It depends on a complex parameter λ, called the *spectral parameter*. It can be shown explicitly that the Lax operator fulfills the commutator relations

$$\check{R}(\lambda-\mu)\big(L_n(\lambda) \otimes L_n(\mu)\big) = \big(L_n(\mu) \otimes L_n(\lambda)\big)\check{R}(\lambda-\mu) \tag{2.31}$$

the 4×4 matrix $\check{R}$ being defined as

$$\check{R}(\lambda) = \frac{1}{\lambda+\mathrm{i}}\Big((\frac{\lambda}{2}+\mathrm{i})\mathbb{I}\otimes\mathbb{I} + \frac{\lambda}{2}\sum_{\alpha=x,y,z}\sigma^\alpha \otimes \sigma^\alpha\Big). \tag{2.32}$$

Sometimes it is convenient to separate a permutation, $\check{R} = PR$, where the permutation operator P interchanges the two products of the tensor space $\mathbb{C}^2 \otimes \eta_n$ on which $\check{R}$ is defined. Both matrices are usually referred to simply as *the R-matrix*. In the standard basis of $\mathbb{C}^2$ it takes the form

$$\check{R}(\lambda) = \begin{pmatrix} 1 & 0 & 0 & 0 \\ 0 & c(\lambda) & b(\lambda) & 0 \\ 0 & b(\lambda) & c(\lambda) & 0 \\ 0 & 0 & 0 & 1 \end{pmatrix}, \tag{2.33}$$

where the functions $b(\lambda)$ and $c(\lambda)$ must be defined differently for the XXX model and the XXZ model,

$$\begin{array}{ll} \text{XXX} & \text{XXZ} \\ b(\lambda) = \frac{\lambda}{\lambda+\mathrm{i}} & b(\lambda) = \frac{\sinh(\lambda)}{\sinh(\lambda+\eta)} \\ c(\lambda) = \frac{\mathrm{i}}{\lambda+\mathrm{i}} & c(\lambda) = \frac{\sinh(\eta)}{\sinh(\lambda+\eta)} \end{array} \tag{2.34}$$

The anisotropy of the XXZ model is parameterized as $\Delta = \cosh\eta$. The Lax operator serves mainly as a step towards the so-called monodromy matrix

$$\mathcal{T}(\lambda) = L_N(\lambda)L_{N-1}(\lambda)\cdots L_1(\lambda) = \begin{pmatrix} A(\lambda) & B(\lambda) \\ C(\lambda) & D(\lambda) \end{pmatrix} \tag{2.35}$$

which by construction inherits the commutation relation (2.31),

$$\check{R}(\lambda-\mu)(\mathcal{T}(\lambda)\otimes\mathcal{T}(\mu)) = (\mathcal{T}(\mu)\otimes\mathcal{T}(\lambda))\check{R}(\lambda-\mu). \tag{2.36}$$

The name *monodromy matrix* stems from a connection between the Lax operator and the permutation operator. Since the Lax operator acts basically as the permutation of η_n and η_{n+1}, the monodromy matrix has this transposition run once through the whole Hilbert space. With the application on physical models with periodic boundary conditions in mind this transposition runs a full circle. This idea is precisely defined in topology where a monodromy is the run around a singularity. The entries of the monodromy matrix act, of course, on the Hilbert space. The trace of the monodromy matrix is called the *transfer matrix*,

$$T(\lambda) = \operatorname{tr}\mathcal{T}(\lambda) = A(\lambda) + D(\lambda), \tag{2.37}$$

and acts on the Hilbert space $\mathcal{H}_N$, too. It is easy to show that the transfer matrices commute for all values of the spectral parameter,

$$[T(\lambda), T(\mu)] = 0 \quad \forall\lambda,\mu\in\mathbb{C}. \tag{2.38}$$

This is of great importance to the physical problem, since (in a broader sence) among these family of commutating operators are the momentum operator P and the Hamilton operator H, although the connection is intricate,

$$P = -\mathrm{i}\ln\big((-\mathrm{i})^N T((\mathrm{i}/2)\big), \qquad H = \frac{\mathrm{i}J}{2}\Big(\frac{\mathrm{d}}{\mathrm{d}\lambda}\ln T(\lambda)\Big)_{\lambda=\mathrm{i}/2}. \tag{2.39}$$

Therefore H and $T(\lambda)$ have a common system of eigenvectors. These can be constructed beginning with a *highest weight vector*

$$|\Omega\rangle = \bigotimes_{n=1}^{N}\begin{pmatrix} 1 \\ 0 \end{pmatrix}_n \tag{2.40}$$

being eigenvector of the operators A and D,

$$A(\lambda)|\Omega\rangle = a(\lambda)|\Omega\rangle, \qquad C(\lambda)|\Omega\rangle = 0, \qquad D(\lambda)|\Omega\rangle = d(\lambda)|\Omega\rangle. \tag{2.41}$$

Physically speaking $|\Omega\rangle$ is the ferromagnetic ground state. All other eigenstates of the system can be generated from $|\Omega\rangle$ by multiply applying the operator B. For this reason the operators B and C are named creation and annihilation operator, respectively. It follows from the commutation relations for the operators A, B, C, D, that the vector

$$|\Psi(\lambda_1,\ldots,\lambda_r)\rangle = B(\lambda_1)\ldots B(\lambda_r)|\Omega\rangle \tag{2.42}$$

is an eigenvector of the family of commuting operators (2.38) and (2.39) for every set of parameters $\{\lambda_j\}$ satisfying the system of equations

$$\frac{d(\lambda_j)}{a(\lambda_j)} = \prod_{\substack{k=1\\k\neq j}}^{r}\frac{c(\lambda_j-\lambda_k)}{c(\lambda_k-\lambda_j)}, \qquad j=1,\ldots,r. \tag{2.43}$$

The functions $a(\lambda)$ and $d(\lambda)$ can be obtained from (2.41) since the vacuum state $|\Omega\rangle$ is explicitly known. In the XXZ case they are given by

$$a(\lambda) = 1, \qquad d(\lambda) = b^N(\lambda) = \left(\frac{\sinh\lambda}{\sinh(\lambda+\eta)}\right)^N \tag{2.44}$$

and Eqs. (2.43) become

$$\left(\frac{\sinh\lambda_j}{\sinh(\lambda_j+\eta)}\right)^N = \prod_{\substack{k=1\\k\neq j}}^{r} \frac{\sinh(\lambda_k-\lambda_j+\eta)}{\sinh(\lambda_j-\lambda_k+\eta)}, \qquad j=1,2,\ldots,r. \tag{2.45}$$

In the shifted variables $\lambda_j^{'} = \lambda_j + \eta/2$ these are exactly the Bethe ansatz equations (2.25). The corresponding eigenvalue of $|\Psi\rangle$ is found to be

$$\begin{aligned}\Lambda(\lambda) &= a(\lambda)\prod_{j=1}^{r}\frac{1}{c(\lambda_j-\lambda)} + d(\lambda)\prod_{j=1}^{r}\frac{1}{c(\lambda-\lambda_j)} \\ &= \prod_{j=1}^{r}\frac{\sinh(\lambda_j-\lambda-\eta)}{\sinh\eta} + \left(\frac{\sinh(\lambda_j-\lambda)}{\sinh(\lambda_j-\lambda-\eta)}\right)^N \prod_{j=1}^{r}\frac{\sinh(\lambda-\lambda_j+\eta)}{\sinh\eta}.\end{aligned} \tag{2.46}$$

We have tacitly assumed that the creation operator B generates the whole spectrum. This question has been analyzed in depth by Fabricius et. al. [26, 27].

2.4 Dynamic Spin Structure Factors

The ground state of the XXZ model can be understood as the spinonic vacuum[2] if the system size N is even. In any case the excitations can be generated by systematic creation of spinon pairs (see [17, 28] and references therein). Theoretical as well as experimental results suggest that for sufficiently low temperatures the excitations of only a few spinons govern the spin dynamics of the model (see again [17] and references therein).

But calculating the corresponding spin structure factors has been an open problem for decades. Important milestones along the way are the work of Korepin [29] in 1982, Slavnov [30] in 1989 and the Lyon group around Kitanine and Maillet [16] in 1999. They showed how to reduce (i) the norm of Bethe wave functions [29] and (ii) the scalar products of the wave vectors [30] and (iii) the form factors of local spin operators to determinants [16]. The axial regime $|\Delta| > 1$ was analyzed in 1997 by Karbach et al. [31] and the planar regime $|\Delta| < 1$ has been discussed by Biegel et al. in 2003 [17]. They used the determinantal expressions from [16] to calculate transition rates for in-plane dynamic spin structure factors. This section briefly refers their results which will be specialized to the XX model in Sec. 3.4.

The low-temperature spin dynamics are dominantly governed by the dynamic spin structure factor for spin fluctuations. This means that the dynamic spin structure factor completely describes the non-trivial part of the corresponding part of the partial differential cross-section for neutron scattering and thus relates the theoretical results to experimental analysis. We have established this connection in App. E.

The underlying transition of the system is described by the action of the spin fluctuation operator

$$S_q^\mu = \frac{1}{\sqrt{N}}\sum_{n=1}^{N} \mathrm{e}^{\mathrm{i}qn} S_n^\mu, \qquad \mu \in \{+,-,z\}, \tag{2.47}$$

[2] The definition of spinons (some quasiparticles) will be given in Sec. 3.3.

where the operator S_n^z probes the z-component of the spin on the n^{th} lattice site and $S_n^\pm$ are the local spin flip operators. The parameter $q = k_f - k_i$ is the difference between the total momentum[3] of the final and the initial state. The fluctuation operator S_q^μ probes the spin fluctuation parallel ($\mu = z$) and perpendicular ($\mu = \pm$) to the quantization axis z. At zero temperature the probability for the transition is given by the transition rate

$$M_\lambda^\mu(q) = \frac{\left|\langle\psi_0|S_q^\mu|\psi_\lambda\rangle\right|^2}{\|\psi_0\|^2\,\|\psi_\lambda\|^2}, \qquad \mu \in \{+,-,z\} \tag{2.48}$$

from the ground state $|\psi_0\rangle$ to the excited state $|\psi_\lambda\rangle$. The transition rate for the perpendicular spin fluctuations has been reported in [17] to be

$$M_\lambda^\pm(q) = N\left(\frac{\mathcal{L}_r(\{z_i^0\})}{\mathcal{L}_{r\pm1}(\{z_i\})}\right)^{\pm1} \mathcal{K}_r(\{z_i^0\})\mathcal{K}_{r\pm1}(\{z_i\})\frac{|\det \mathsf{H}^\pm|^2}{\det \mathsf{K}(\{z_i\})\det \mathsf{K}(\{z_i^0\})}. \tag{2.49}$$

The matrices are given by

$$\begin{aligned}
\mathsf{H}^+_{a,b} &= \frac{\mathrm{i}}{2}\,\frac{\sin\gamma}{\sinh[(z_a - z_b^0)/2]}\left(\prod_{j\neq a}^{r+1} G(z_j - z_b^0) - d(z_b^0)\prod_{j\neq a}^{r+1} G^\star(z_j - z_b^0)\right)\\
\mathsf{H}^+_{a,r+1} &= \mathrm{i}\kappa(z_a), \qquad a = 1,\ldots,r+1,\ b = 1,\ldots,r \qquad (2.50)\\
\mathsf{H}^-_{a,b} &= \frac{\mathrm{i}}{2}\,\frac{\sin\gamma}{\sinh[(z_a^0 - z_b)/2]}\left(\prod_{j\neq a}^{r} G(z_j^0 - z_b) - d(z_b)\prod_{j\neq a}^{r} G^\star(z_j^0 - z_b)\right)\\
\mathsf{H}^-_{a,r} &= \mathrm{i}\kappa(z_a^0), \qquad a = 1,\ldots,r,\ b = 1,\ldots,r-1 \qquad (2.51)\\
\mathsf{K}_{a,b} &= \begin{cases} K(z_a - z_b)\cos\gamma & :\ a \neq b \\ N\kappa(z_a) - \cos\gamma\sum_{j\neq a}^r K(z_a - z_j) & :\ a = b \end{cases} \qquad (2.52)
\end{aligned}$$

and the functions G, d, κ, and K are

$$\begin{aligned}
G(z) &= \sinh(z/2)\cot\gamma + \mathrm{i}\cosh(z/2), \qquad (2.53)\\
d(z) &= \left(\frac{\tanh(z/2)\cot(\gamma/2) - \mathrm{i}}{\tanh(z/2)\cot(\gamma/2) + \mathrm{i}}\right)^N, \qquad (2.54)\\
\kappa(z) &= \frac{1}{2}\,\frac{\sin^2\gamma}{\sinh^2(z/2) + \sin^2(\gamma/2)}, \qquad (2.55)\\
K(z) &= \frac{\sin^2\gamma}{\sinh^2(z/2) + \sin^2\gamma}, \qquad (2.56)
\end{aligned}$$

respectively. Throughout this section the anisotropy is parameterized by

$$\Delta = \cos\gamma \tag{2.57}$$

and the z-component of the total spin is written as

$$S_T^z = \frac{N}{2} - r. \tag{2.58}$$

[3] Strictly speaking k_i and k_f are wave numbers since the calculation is done in Fourier space on the reciprocal lattice.

Once the transition rate is available, the corresponding dynamic spin structure factors

$$S_{\mu\nu}(q,\omega) = 2\pi \sum_{\lambda} M_{\lambda}^{-}(q)\delta(\omega - \omega_{\lambda}), \qquad \mu,\nu \in \{+,-,z\} \tag{2.59}$$

can be calculated. Here, $\omega_\lambda = E_\lambda - E_0$ is the energy difference between the two involved states. The sum runs over all 2^N states of the system.
Usually the excitations are grouped and the sum is (analytically or numerically) carried out over certain selected classes only. We will classify the states for the XX model by their spinon content (see Sec. 3.3). Then we will obtain analytic expressions for the experimentally relevant classes with up to four spinons in Sec. 3.4.

3 The XX Model

The XX model is the critical point $\Delta = 0$ of vanishing anisotropy of the XXZ model (2.5) which makes all results of the previous section available for this special case. The adoption of the Bethe ansatz leads to a description of the spectrum in terms of quasi-particles named *magnons*. We will use the Bethe ansatz solution in Chapter 3.1 to classify all XX eigenstates.
From the analytical point of view the great importance of the XX model lies in the fact that it is equivalent to a model of spinless free hardcore lattice fermions[4]. The XX Hamiltonian can be mapped onto the Hamiltonian of the free fermion gas by a so-called Jordan-Wigner transformation [32] as was first observed by Lieb et. al. [33]. In this approach the spectrum can be generated in terms of free fermions. Many results have been derived thus because the fermions are non-interacting.
But in both descriptions the ground state and the energetically low-lying excitations are populated by a huge number of quasi particles. It is this number of quasi particles (typically of the order of the lattice size N) which strongly limits the numerical access to many interesting quantities such as structure factors and other correlation functions. A way out has been found by the introduction of yet another type of quasi-particles, the so-called *spinons*, which have recently been introduced for the XX-model [34].

3.1 Magnons

In Sec. 2.2 we have demonstrated how the XXZ model can be solved by the coordinate Bethe ansatz. All states can be characterized by sets of solutions of the Bethe ansatz equations (2.26) and are parameterized by a set of Bethe quantum numbers $\{I_i\}$. In the XX limit the Bethe ansatz equations simplify drastically. The limit $\Delta \to 0$ implies $c_1 \to 0$ und $c_2 \to 1$ and thus leads to the trivial equations

$$y_i = \tan\left(\frac{\pi I_i}{N}\right) \quad \Longleftrightarrow \quad k_i = \pi - \frac{2\pi I_i}{N}, \quad i = 1, 2, \ldots, r. \tag{3.1}$$

The variables k_i are interpreted as *magnon momenta* and the parameters I_i are their momentum quantum numbers. The XX limit of the Bethe ansatz equations was analyzed in detail in a previous study [18]. There it was demonstrated that (3.1) holds only under the restriction that among the solutions of (2.26) there is no pair $y_i(\Delta)$, $y_j(\Delta)$ with the limit $y_i(0)y_j(0) = 1$ or equivalently $k_i(0)k_j(0) = \pi$. These pairs are called *critical pairs*. We will explain how to circumnavigate all technical problems caused by them in Sec. 3.4.1.
In the XX limit the Bethe quantum numbers are integers for odd r and half-integers for even r where the parameter r is related to the magnetization via (2.9). They are confined to the range $|I_i| \leq N/2$. The energy of any state is given by

$$E = \sum{}' \cos k_i \tag{3.2}$$

where the sum includes non-critical momenta only. The wave number of a generic state with arbitrarily many real and complex conjugated critical pairs can be found in [18]. We do not discuss the complications of critical pairs any further but refer to Sec. 3.4.1 where we explain how to circumnavigate the arising problems.
In the formalism of the thermodynamic Bethe ansatz it is possible to derive the thermodynamic properties from magnons, which we will not discuss here. Instead we give the well-known results in the fermionic language (see Sec. 3.2.2). In Sec. 3.3.5 we will demonstrate how thermodynamics can alternatively be formulated in the spinonic language which was not known before.

[4] The quasiparticles are fermionic in the sence that each state can be occupied by at most one particle. The attribute "spinless" means that no spin interaction is present.

3.2 Fermions

3.2.1 Basic Properties

The Hamiltonian of the XX model is the limit $\Delta \to 0$ of the XXZ model, namely

$$\mathcal{H}_{\mathrm{XX}} = J \sum_{i=1}^{N} \left(S_i^x S_{i+1}^x + S_i^y S_{i+1}^y \right) = \frac{J}{2} \sum_{i=1}^{N} \left(S_i^+ S_{i+1}^- + S_i^- S_{i+1}^+ \right). \tag{3.3}$$

By means of a Jordan-Wigner transformation and a Fourier transformation to the reciprocal lattice the Hamiltonian (3.3) is brought into the form

$$\mathcal{H}_{\mathrm{XX}} = \sum_{\{p_i\}} \cos(p_i) c_{p_i}^\dagger c_{p_i} \tag{3.4}$$

where $c_p^\dagger$ and c_p are fermion creation and annihilation operators. The allowed fermion momenta p_i are given by

$$p_i = \frac{\pi \bar{m}_i}{N}, \qquad \begin{array}{ll} \bar{m}_i \in \{1, 3, \ldots, 2N-1\} & \text{for even } N_f \\ \bar{m}_i \in \{0, 2, \ldots, 2N-2\} & \text{for odd } N_f \end{array} \tag{3.5}$$

where the number of fermions lies in the range $0 \leq N_f \leq N$. Fermions are computationally convenient because they are spinless and do not interact. The energy of any state is simply given by

$$E = \sum_{\{p_i\}} \cos(p_i). \tag{3.6}$$

We will always write p for the fermion momenta and reserve the letters k and κ for spinon momenta.

3.2.2 Thermodynamics

The thermodynamics of the XX model has been derived in the fermion formalism by Katsura [35] in 1962. There the anisotropic XY model with an external magnetic field in z direction was analyzed. We will briefly sketch how the XX-result can be obtained elementarily.
In general, the total energy and the fermionic particle content of the system are not kept fixed. Thus the grand canonical ensemble is most suitable. The starting point is the grand partition function [36]

$$Z(\mu, \beta) = \prod_i \left(1 + z \mathrm{e}^{-\beta \epsilon_i} \right) \tag{3.7}$$

the fugacity being defined by $z = \exp(\beta\mu)$ where μ is the chemical potential. We use the inverse temperature $\beta = 1/(k_B T)$ which has the dimension of energy. The dispersion relation can be inferred from Eq. (3.6) with $\epsilon_i = \cos p_i$. Thus the grand partition function becomes

$$Z(\mu, \beta) = \prod_{p_i} \left[1 + \mathrm{e}^{\beta(\mu - \cos p_i)} \right]. \tag{3.8}$$

Taking the logarithm yields the free energy

$$F(\mu, T) = -k_B T \ln(Z) = -k_B T \sum_{p_i} \ln \left[1 + \mathrm{e}^{\beta(\mu - \cos p_i)} \right]. \tag{3.9}$$

In the thermodynamic limit $N \to \infty$ the sum will become an integral and the discrete fermion momenta p_i will become a continuous variable $0 \leq p \leq 2\pi$:

$$p_i \to p, \qquad \sum_{p_i} \to \int_0^{2\pi} \mathrm{d}p\, \rho(p) = N \int_0^{2\pi} \frac{\mathrm{d}p}{2\pi}. \tag{3.10}$$

From (3.5) we infer the distribution function $\rho(p) = N/(2\pi)$ of the possible fermion momenta. Then the free energy per site of the infinite chain is

$$f(\mu, T) = \lim_{N\to\infty} \frac{1}{N} F(\mu, T) = -k_B T \int_0^{2\pi} \frac{\mathrm{d}p}{2\pi} \ln\left[1 + \mathrm{e}^{\beta(\mu - \cos p)}\right]. \tag{3.11}$$

Since the integration is performed over a full period of the cosine function it is possible to shift the limits of integration by an arbitrary offset. We choose $-\pi$ and rewrite the argument of the logarithm for later convenience,

$$\begin{aligned} f(\mu, T) &= -k_B T \int_{-\pi}^{+\pi} \frac{\mathrm{d}p}{2\pi} \ln\left[1 + \mathrm{e}^{\beta(\mu - \cos p)}\right] && (3.12)\\ &= -k_B T \int_{-\pi}^{+\pi} \frac{\mathrm{d}p}{2\pi} \ln \frac{2\cosh\frac{\beta}{2}(\mu - \cos p)}{\exp -\frac{\beta}{2}(\mu - \cos p)} \\ &= -\frac{1}{2}\mu - k_B T \int_{-\pi}^{+\pi} \frac{\mathrm{d}p}{2\pi} \ln\Big(2\cosh\frac{\beta}{2}(\mu - \cos p)\Big). && (3.13) \end{aligned}$$

The Gibbs free energy is given by

$$\begin{aligned} g(\mu, T) &= f(\mu, T) + \mu n_f - h m_z && (3.14)\\ &= h\Big(\frac{1}{2} - n_f - m_z\Big) - k_B T \int_{-\pi}^{+\pi} \frac{\mathrm{d}p}{2\pi} \ln\Big(2\cosh\frac{\beta}{2}(h + \cos p)\Big) && (3.15) \end{aligned}$$

where we have translated the chemical potential into the external magnetic field by setting $\mu = -h$. The term $(\frac{1}{2} - n_f - m_z)$ is identically zero by a connection between the magnetization and the number of fermions which will be shown in Eq. (3.26) in Sec. 3.3.2. Hence we obtain

$$g(\mu, T) = -k_B T \int_{-\pi}^{+\pi} \frac{\mathrm{d}p}{2\pi} \ln\Big(2\cosh\frac{\beta}{2}(h + \cos p)\Big) \tag{3.16}$$

in accordance with [35]. We will show in Sec. 3.3.5 how this result can be derived in the spinon picture as well.

3.3 Spinons

3.3.1 Definition

It has been known for a long time that the basic excitations of the Heisenberg model are of spin one half. Important work has been done by Faddeev and Takhtadzhan [15, 28, 37] on that frontier.

These quasiparticles, nowadays called spinons, have also been found by Haldane [38] in a derivative of the Heisenberg model with inverse-square interaction now called Haldane-Shastry model. There the spinons have been analyzed explicitly for the first time.
In [34] we have shown in greater detail how to describe the spectrum of the XX model as a composite of spinon states. Here we will give an even slightly more detailed explanation using the original figures from [34].
Initially, quasiparticles in general are nothing more but a way of labeling all states of the spectrum. We start with the well-known fermionic description of the spectrum and introduce a relabelling via a one-to-one mapping from the spectrum onto itself. This mapping will be described by two sets of numbers which are conveniently named spinon momentum quantum numbers and spinon spin quantum numbers.
First, we give this mapping so as to define the spinons. Only afterward will we interpret the spinons as quasiparticles carrying physical properties.
The proceeding must be done for systems of odd and even size differently.

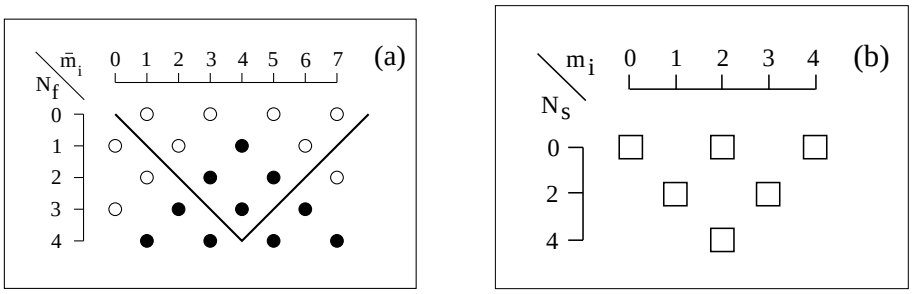

Figure 1: (a) Fermion momentum states available to N_f fermions and (b) spinon momentum states available to N_s spinons in XX eigenstates for $N = 4$. All momenta are in units of π/N. Fermion momentum states can be either vacant (open circle) or singly occupied (full circle). The particular fermion configuration shown in each row represents the lowest energy state for given N_f. Spinon momentum states can be either vacant or occupied by up to N_s spinons with arbitrary spin polarization. No specific spinon configuration is shown.

1. Spinons in an even-sized system We illustrate the mapping between fermion and spinon states in a system of size $N = 4$ but the generalization to an arbitrary even number N is obvious.

   Part (a) of Fig. 1 shows the allowed fermion momentum states (open and full circles) according to Eq. (3.5). The set of circles is divided into two parts by a $\vee$-shaped line. The part above this line is named the *inside* and the part below is named the *outside*. The outside is understood to be periodically closed at $\bar{m}_i = 2N = 0$.

   All 2^N states are obtained if for every allowed number of fermions, $0 \leq N_f \leq N$, all possible momentum distributions are taken. Thus any state can be described as a list of fermionic momenta $\bar{m}_i$.

   In the spinonic language, every state shall be described as a list of N_s spinons with spinon momenta m_i and spinon spins σ_i. The spinon spin quantum number takes only two values which are arbitrarily chosen to be $+1$ and -1. The spins are commonly referred to as up-spins and down-spins, respectively.

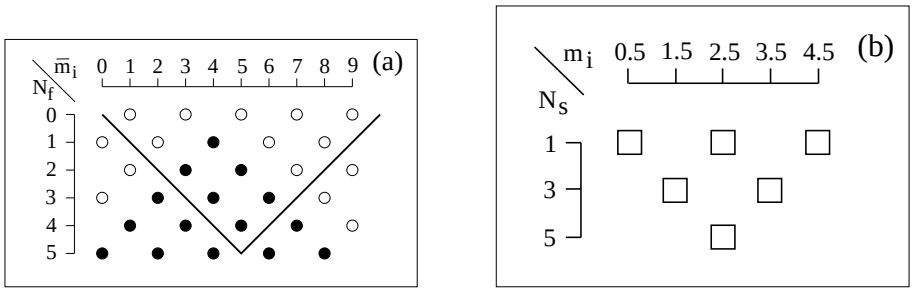

Figure 2: (a) Fermion orbitals available to N_f fermions and (b) spinon orbitals available to N_s spinons in XX eigenstates for $N = 5$. Fermion orbitals can be either vacant (open circle) or singly occupied (full circle). The particular fermion configuration shown in each row represents one of two lowest energy states for given N_f. Spinon orbitals can be either vacant or occupied by up to N_s spinons with arbitrary spin polarization. No specific spinon configuration is shown.

Now every fermionic hole (open circle) inside represents a spin-up spinon and every fermionic particle (full circle) outside represents a spin-down spinon. Thus the polarization (total spin) and number of spinons of the corresponding spinon state is determined.

The possible values for the momentum are given in Fig. 1(b). For determining the actual momentum values we read Fig. 1(a) line by line from left to right starting at the left prong of the $\vee$. All consecutive fermionic holes in the inside represent spinons in the same momentum state and every interlaying fermion increases the momentum of the following spinons by $2\pi/N$. If the first spinon state right of the left prong is vacant the corresponding spinon momentum takes the lowest possible value according to Fig. 1(b). Starting with the right prong and runnig through the outside the momenta of the spin-down spinons are determined in the same way, where only the roles of fermionic particles and holes are interchanged. To illustrate this construction we give the full spectrum for $N = 4$ in the fermionic and the spinonic language in Fig. 3.

2. Spinons in an odd-sized system Again we illustrate the mapping between fermion and spinon states in a small system ($N = 5$ this time). The possible momenta are encoded in Fig. 2. Subfigure (a) gives all possible fermionic momenta and subfigure (b) all spinon momenta. The mapping between the fermionic and spinonic description is analogous to the case of even N. We perform the same steps and the only difference lies in the slightly shifted[5] spinon momenta m_i. An expanded version of Fig. 2 is shown in Fig. 4 with all 2^5 quantum states. The ground state is fourfold degenerate and contains one spinon, located at either side of either prong of the fork. This structure holds for arbitrary odd N.

For a system of arbitrary (even or odd) size N, the allowed values for the spinon momenta as given in Fig. 1 and 2 are

$$\kappa_i = \frac{\pi m_i}{N}, \qquad m_i \in \left\{ \frac{N_s}{2}, \frac{N_s}{2} + 2, \ldots, N - \frac{N_s}{2} \right\} \tag{3.17}$$

where the number of spinons can take the values

$$N_s = \begin{cases} 0, 2, \ldots, N & \text{for even } N \\ 1, 3, \ldots, N+1 & \text{for odd } N \end{cases} . \tag{3.18}$$

[5] The notation has changed from [34] to [39]. In this work we use the latter convention.

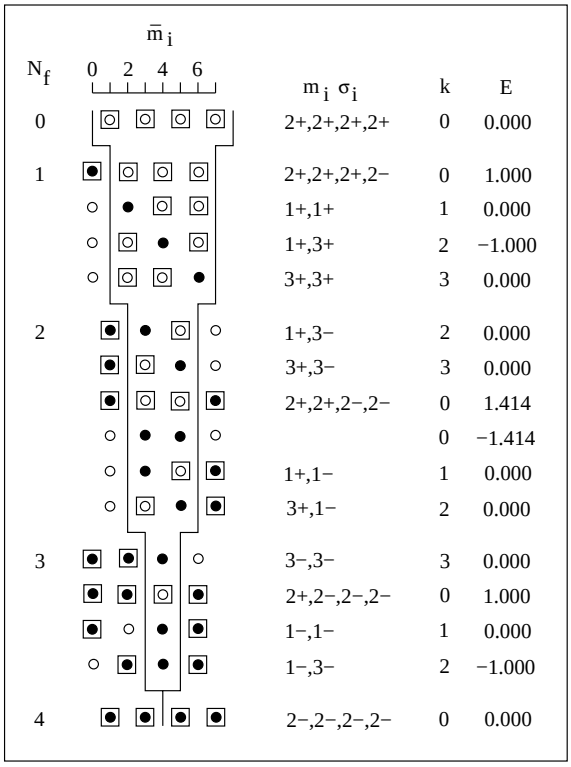

Figure 3: Fermion configurations of all eigenstates for $N = 4$. Fermionic particles (holes) are denoted by full (open) circles. Spinon particles with spin up (down) are denoted by squares around open (full) circles. The fermion momenta $\bar{m}_i$ (in units of π/N) can be read off the diagram. The spinon momenta m_i (also in units of π/N) and the spinon spins σ_i are given explicitly and can be inferred from the fermion configuration as explained in the text. Also given are the wave number k (in units of $2\pi/N$) and the energy E of each eigenstate.

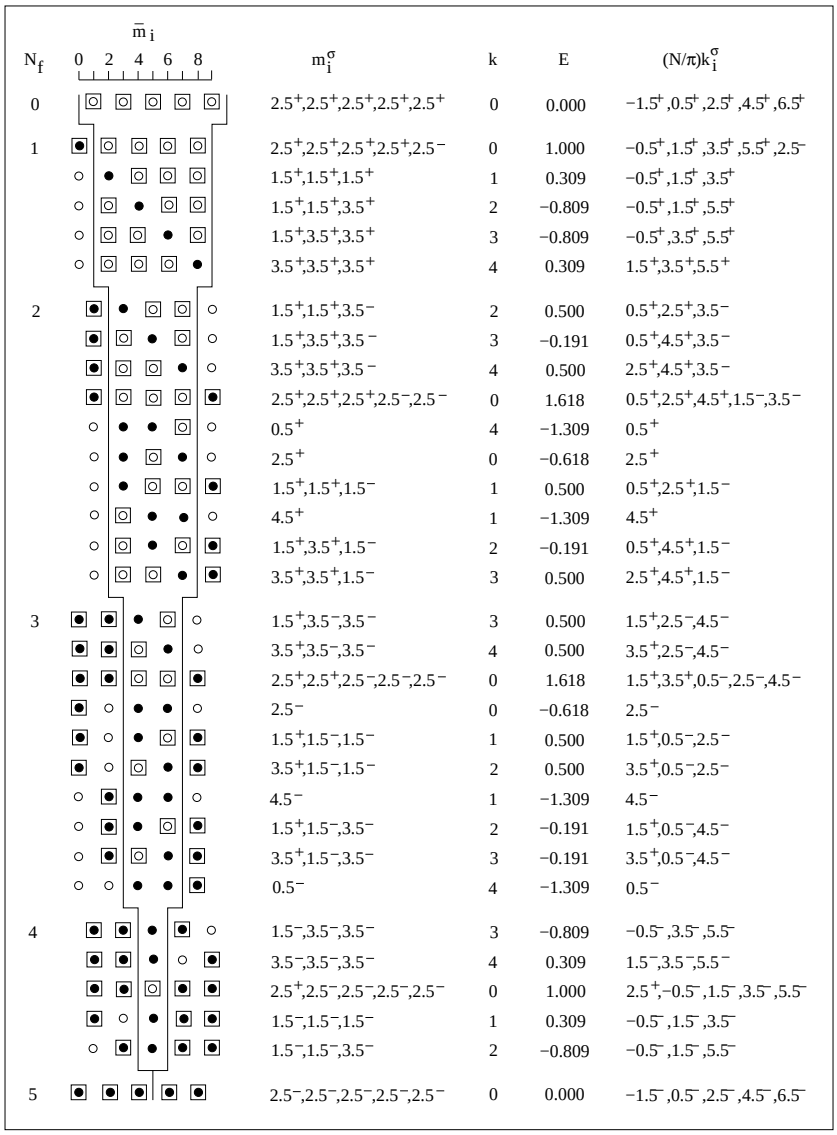

Figure 4: Fermion configurations of all eigenstates for $N = 5$. Fermionic particles (holes) are denoted by full (open) circles. Spinon particles with spin up (down) are denoted by squares around open (full) circles. The fermion quantum numbers $\bar{m}_i$ can be read off the diagram. The spinon quantum numbers m_i^σ are given explicitly and can be inferred from the fermion configuration as explained in the text. Additionally we give the wave number k (in units of $2\pi/N$) and the energy E of each XX eigenstate. The spinon momenta k_i^σ are discussed in Sec. 3.3.3.

3.3.2 Interaction

If a quantum state with N_f fermion quantum numbers $\bar{m}_i$ is given, the mapping described in Sec. 3.3.1 generates a unique set of N_s spinon quantum numbers. We denote the number of up and down spinons by N_+ and N_-, respectively. The quantum numbers of up and down spinons must not be confused. We therefore label them with a superscript '+' or '−'. Those with the same label are enumerated in ascending order,

$$\frac{N_s}{2} \leq m_1^\sigma \leq m_2^\sigma \leq \cdots \leq m_{N_\sigma}^\sigma \leq N - \frac{N_s}{2}, \quad \sigma = \pm. \tag{3.19}$$

We calculate the number of different spinon configurations. First, we note that the number of possible momentum values is $A = 1 + (N - N_s)/2$ for up- and down-spinons each. Let us now introduce a set of occupancy numbers $c_1, c_2, \ldots, c_A$ for the up-spinons. So c_k is the number of quantum numbers m_i^+ taking the k^{th} possible value, which is $N_s/2+2(k-1)$. The occupancy numbers are, of course, natural numbers confined to the interval $0 \leq c_k \leq N_+$ and are subject to the constraint $c_1 + \ldots + c_A = N_+$. The number of such partitions is known to be $\binom{A+N_+-1}{N_+}$. The number of down-spionon configurations is obviously the same with N_+ replaced by N_-. We thus obtain the number of states containing N_s spinons N_+ of which carry up-spin:

$$P(N, N_s, N_+) = \binom{A + N_+ - 1}{N_+}\binom{A + N_- - 1}{N_-}. \tag{3.20}$$

The number of states containing N_s spinons is obtained by summing over N_+,

$$\sum_{N_+=0}^{N_s} P(N, N_s, N_+) = \binom{N+1}{N_s}. \tag{3.21}$$

Details of the calculation can be found in Appendix C. Summing over N_s yields 2^N so that indeed all states are accounted for.
The energy of any eigenstate can be written in terms of the spinon momentum quantum numbers:

$$E\big(\{m_{j_+}^+\}, \{m_{j_-}^-\}\big) = E_0(N_+, N_-) + \sum_{\sigma=\pm} \sum_{j_\sigma=1}^{N_\sigma} \sin\left(\kappa_{j_\sigma}^\sigma - \tau_{j_\sigma}^\sigma\right) \tag{3.22}$$

with

$$\kappa_{j_\sigma}^\sigma = \frac{\pi}{N}\, m_{j_\sigma}^\sigma, \quad \tau_{j_\sigma}^\sigma = \frac{\pi}{N}\big(N_\sigma + 1 - 2j_\sigma\big), \quad \sigma = \pm. \tag{3.23}$$

The reference energy

$$E_0(N_+, N_-) = \sum_{\{\bar{m}_i^0\}} \cos\left(\frac{\pi}{N}\,\bar{m}_i^0\right), \tag{3.24}$$

$$\{\bar{m}_i^0\} = \left\{\frac{1}{2}(N + N_+ - N_- + 2), \frac{1}{2}(N + N_+ - N_- + 6), \ldots, \frac{1}{2}(3N - N_+ + N_- - 2)\right\}, \tag{3.25}$$

depends only on $N_+ - N_-$, i.e., the magnetization

$$M_z = \frac{N}{2} - N_f = \frac{N_+ - N_-}{2}. \tag{3.26}$$

For even N, E_0 is the energy of the lowest eigenstate for given M_z, but for odd N it does not represent the energy of any eigenstate. Eq. (3.22) at the first glance looks like the interaction of free particles

since no interaction is directly implemented. But it enters nevertheless via the sorting criterion (3.19). Changing any spin affects all terms in the sum and changing a single momentum quantum number might alter many terms.

3.3.3 Bethe Ansatz Equations

The energy formula (3.22) looks rather like a coordinate Bethe ansatz equation. It would then describe quasiparticles in a two-body interaction potential. We might very well interpret the spinon momentum quantum numbers m_i as Bethe quantum numbers. And we can even think of the argument of the sine function in (3.22) as the corresponding "true" spinon momentum. Then all spinons of either polarization have distinct momenta,

$$k_{j_\sigma}^\sigma = \frac{\pi}{N}\left(m_{j_\sigma}^\sigma - N_\sigma - 1 + 2j_\sigma\right), \quad j_\sigma = 1, \ldots, N_\sigma, \quad \sigma = \pm. \tag{3.27}$$

The spinon dispersion becomes $\epsilon(k) = \sin k$ and the energy expression (3.22) simplifies to

$$E\big(\{m_{j_+}^+\}, \{m_{j_-}^-\}\big) = E_0(N_+, N_-) + \sum_{\sigma=\pm} \sum_{j_\sigma=1}^{N_\sigma} \sin k_{j_\sigma}^\sigma. \tag{3.28}$$

The long known coordinate Bethe ansatz produces magnon momenta as solutions of the Bethe ansatz equations. If spinons are the outcome of a different Bethe ansatz calculation, the spinon momenta (3.27) should be the solution of an appropriate spinonic Bethe ansatz equation. And indeed we can construct such a system of equations. Insertion shows that the momenta (3.27) are the solutions of the Bethe ansatz like equations

$$Nk_i^\sigma = \pi m_i^\sigma + \sum_{\sigma'=\pm} \sum_{j=1}^{N_{\sigma'}} \theta_{XX}(k_i^\sigma - k_j^{\sigma'}), \quad i = 1, \ldots, N_\sigma, \quad \sigma = \pm, \tag{3.29}$$

$$\theta_{XX}(k_i^\sigma - k_j^{\sigma'}) = \pi \operatorname{sgn}(k_i^\sigma - k_j^{\sigma'})\delta_{\sigma\sigma'}. \tag{3.30}$$

The Kronecker delta reflects the fact that only spinons with parallel spin scatter off each other. The momenta are bounded by

$$\frac{\pi}{N}\left(\frac{1}{2}N_s - N_\sigma + 1\right) \leq k_1^\sigma < k_2^\sigma < \cdots < k_{N_\sigma}^\sigma \leq \frac{\pi}{N}\left(N - \frac{1}{2}N_s + N_\sigma - 1\right). \tag{3.31}$$

The distance of any k_i^σ from the upper or lower bound is $\ell(2\pi/N)$, where the parameter ℓ takes the values $\ell = 0, 1, \ldots, (N - N_s)/2 + N_\sigma - 1$.
Having all different momenta the spinons seem to be fermionic particles. But a thorough analysis reveals their semionic character. The statistical interaction coefficient is defined as

$$\Delta d_\sigma = -\sum_{\sigma'=\pm} g_{\sigma\sigma'} \Delta N_{\sigma'}. \tag{3.32}$$

Since the number of available momentum states for a state with $N_s = N_+ + N_-$ spinons present is affected both by the next particle added and by the shifted bounds of the possible momentum states, the statisticle interaction coefficient is $g_{\sigma\sigma'} = 1/2$ for all spin combinations.

3.3.4 Orbital Interaction

We now have two different sets of spinon momenta, namely those generated from the fermion configuration (3.17) and those defined in the context of the Bethe ansatz consideration (3.27). In this section we will analyze the former momenta. They are not distict so that different spinons can carry the same momentum. Changing the position of view we interpret the momenta (3.17) as the momenta of spinon *orbitals* which can be filled by any number of spinons. As long as only one orbital is present (populated with spinons), a closed expression for the energy can be given which depends on the spin polarization in a simple way. Once more than one orbital is populated, the energy expression decomposes into two-orbital interaction terms where the coupling constants depend on all spins in the system.

1. Spinons in One Orbital, $N_s = N$

   The situation of only one orbital can be analyzed in full detail and already exhibits interesting features. Let us first derive the energy of such a state. We start with the states containing $N_s = N$ spinons. The fermionic description is quite simple: As the number of spinons is maximal, there are no fermions in the inside regime and every site in the outside is occupied. The orbital has momentum $\kappa = \pi m/N = \pi/2$ (see Figs. 1 and 2). The $N+1$ possible states differ in their magnetization and fermion content. The state with maximum magnetization, where all spinon spins are aligned and positive, is the fermionic vacuum with the ground state energy $E_0 = 0$.

   Flipping one spinon spin translates into adding one fermion but shifts all fermionic momenta by one unit. It is of technical convenience to flip two spins a time since then the present fermion momenta remain unaltered. The two new-appearing momenta fill in from both sides as can be seen in Fig. 5. The energy of these states follows recursively,

$$E(N_f) = E(N_f - 2) + 2\cos\frac{(N_f - 1)\pi}{N}, \qquad E(0) = 0, \qquad E(1) = 1. \tag{3.33}$$

   The systematic variation of the number of fermions is shown in Fig. 5.

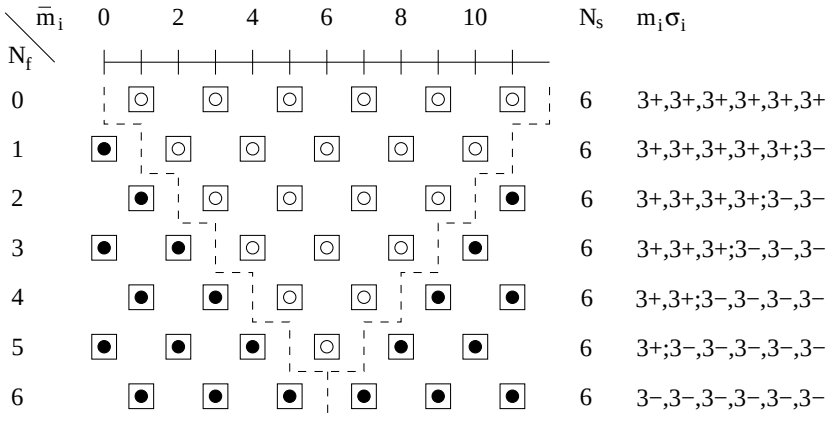

   Figure 5: The picture shows all states with $N_s = N$ spinons for $N = 6$. All spinons are in the same orbital.

   We can derive an explicit expression for the energy in the thermodynamic limit from (3.6). The fermions are evenly spaced over the asymptotic ranges $0 \le \bar{m} \le N_f$ and $2N - N_f \le \bar{m} \le 2N$. We go back to the momenta $p_i = \pi\bar{m}_i/N$ and use the magnetization

$$M_z = \frac{N}{2} - N_f \qquad \Longleftrightarrow \qquad m_z = \frac{1}{2} - n_f \tag{3.34}$$

to obtain the energy as a function of the magnetization,

$$\frac{E(m_z)}{N} = \sum_{i=1}^{2} \int_{p_i^-}^{p_i^+} \frac{\mathrm{d}p}{2\pi} \cos(p) = \frac{1}{2\pi}\big(\sin(p_1^+) + \sin(p_2^+) - \sin(p_1^-) - \sin(p_2^-)\big) = \frac{1}{\pi}\cos(\pi m_z), \tag{3.35}$$

where $p_i^{\pm}$ are the left (-) and right (+) borders of the left ($i = 1$) and right ($i = 2$) range of momenta.

The energy spacing varies between $\Delta E = \mathcal{O}(1)$ at the bottom ($N_f \approx 0$) and $\Delta E = \mathcal{O}\left(N^{-1}\right)$ at the top ($N_f \lesssim N/2$).

2. A Microscopic Model

   This energy distribution can be explained qualitatively by a simple microscopic model for the spinon-spin interaction. We write down the Hamiltonian of a ferromagnetic equivalent-neighbor Ising model,

$$\mathcal{H}_e = -J_e \sum_{i<j} \big(\sigma_i \sigma_j - 1\big), \qquad \sigma_i = \pm 1. \tag{3.36}$$

   The energy-level spectrum of $\mathcal{H}_e$ is

$$E_e = \frac{1}{2} J_e \big(N^2 - (2M_z)^2\big), \quad M_z = \frac{N}{2} - N_f. \tag{3.37}$$

   If we set $J_e = 2/\pi N$ we obtain from (3.37) the following functional dependence for the reduced energy $\epsilon_e = E_e/N$ on the reduced magnetization m_z:

$$\epsilon_e = \frac{1}{\pi}\left(1 - 4m_z^2\right), \qquad -\frac{1}{2} \le m_z \le +\frac{1}{2}. \tag{3.38}$$

   It shares with (3.35) several properties: (i) identical values at $m_z = 0$ and $m_z = \pm 1/2$, (ii) a quadratic dependence at $|m_z| \ll 1/2$, (iii) a linear dependence at $m_z \simeq \pm 1/2$. This qualitatively very good agreement shows that spinons are not sharply localized. They behave rather like equivalently coupled particles with long-range interaction.

3. Spinons in One Orbital, General Case

   We continue to focus on the orbital with momentum $\kappa = \pi/2$ but gradually reduce the number of spinons. The fermion distribution again follows a regular pattern with two groups of fermions along the borders of the inside of the $\vee$. The energy is found to be

$$\epsilon = \frac{1}{\pi}\cos(\pi m_z)\left[2\sin\left(\frac{\pi}{2}\, n_s\right) - 1\right] \tag{3.39}$$

   for $0 \le n_s \le 1$ and $|m_z| \le n_s/2$, in generalization of (3.35). Thinking of the equivalent Ising model, the change affects only the effective interaction strength J_e now depending on n_s. It switches from ferromagnetic interaction for $n_s > 1/3$ to antiferromagnetic interaction for

$n_s < 1/3$. Inspection of those chains, for which the combination of $n_s = 1/3$ and $\kappa = \pi/2$ can be realized, shows that indeed the energy of these states is constantly zero independend of the spin polarization.

If the constraint on the orbital momentum is removed, the generating fermion configuration remains nearly unaltered. The fermions still cluster in three ranges, which are

$$\left\{ \begin{array}{rl} \dfrac{\pi}{2} - \pi m_z \leq & p \leq \dfrac{3\pi}{2} - \dfrac{\pi}{2} n_s - \pi m_z - \kappa \\ \dfrac{3\pi}{2} + \dfrac{\pi}{2} n_s + \pi m_z - \kappa \leq & p \leq \frac{3\pi}{2} + \pi m_z \\ \dfrac{3\pi}{2} - \dfrac{\pi}{2} n_s + \pi m_z + \kappa \leq & p \leq \frac{3\pi}{2} + \frac{\pi}{2} n_s - \pi m_z + \kappa \end{array} \right\} \tag{3.40}$$

with $p = \bar{m}\pi/N$. Integration over these three regions of the fermion energy band $\cos p$ yields

$$\epsilon = \frac{1}{\pi} \cos(\pi m_z) \left[2 \sin\left(\frac{\pi}{2}\, n_s \right) \sin\kappa - 1 \right] \tag{3.41}$$

for $0 \leq n_s \leq 1$, $|m_z| \leq n_s/2$, and $\pi n_s/2 \leq \kappa \leq \pi - \pi n_s/2$. The possible momenta depend on the filling. Or, inverting the inequalities, we can write the maximum capacity as a function of the momentum, $n_s^{\max} = 1 - |1 - 2\kappa/\pi|$.

Speaking in terms of the equivalent Ising model, the interaction strength J_e depends both on the filling n_s and the orbital momentum κ now. As we move away from $\kappa = \pi/2$ to either side, the value of n_s at which the coupling vanishes decreases gradually while the filling $n_s/n_s^{\max}$ increases. At $\kappa = \pi/4$ and $\kappa = 3\pi/4$ we have $J_e = 0$ at $n_s = 1/2$ meaning full capacity ($n_s/n_s^{\max} = 1$). For momenta around zero the coupling is always antiferromagnetic. We see how (3.39) is recovered for $\kappa = \pi/2$ and how (3.35) is then recovered for $n_s = 1$.

4. Spinons in Several Orbitals

Here we discuss the most general scenario: a spinon configuration involving t orbitals with orbital momenta $(\pi/2)n_s \leq \kappa_1 < \kappa_2 < \cdots < \kappa_t \leq \pi - (\pi/2)n_s$ and with the spinon content of each orbital described by the variables

$$\nu_i = \frac{\pi N_s^{(i)}}{2N}, \quad \mu_i = \frac{\pi M_z^{(i)}}{N}, \quad i = 1, 2, \ldots, t; \quad \frac{\pi}{2} n_s = \sum_{i=1}^{t} \nu_i. \tag{3.42}$$

The energy expression for this spinon configuration can be rendered as follows:

$$\begin{aligned} \pi\epsilon \;=\; & \sum_{i=1}^{t-1} \cos\bar{\mu}_{i,i+1} \left\{ \cos\bar{\nu}_{i,i+1} \Big[\cos\kappa_{i+1} - \cos\kappa_i \Big] + \sin\bar{\nu}_{i,i+1} \Big[\sin\kappa_i - \sin\kappa_{i+1} \Big] \right\} \\ & + \cos\bar{\mu}_{t,t+1} \left\{ \cos\bar{\nu}_{t,t+1} \Big[\cos\kappa_1 - \cos\kappa_t \Big] + \sin\bar{\nu}_{t,t+1} \Big[\sin\kappa_1 + \sin\kappa_t \Big] - 1 \right\}, \end{aligned} \tag{3.43}$$

where

$$\bar{\mu}_{i,k} = \sum_{j=1}^{i} \mu_j - \sum_{j=k}^{t} \mu_j, \qquad \bar{\nu}_{i,k} = \sum_{j=1}^{i} \nu_j - \sum_{j=k}^{t} \nu_j. \tag{3.44}$$

The first $t-1$ terms represent a coupling between nearest-neighbor spinon orbitals in orbital momentum space. Each such term depends on the momenta of the two coupled orbitals and on the "local" conserved quantities $\bar{\mu}_{i,i+1}$ and $\bar{\nu}_{i,i+1}$, which play the role of coupling constants for nearest-neighbor orbitals. The last term has a slightly different structure and depends on the smallest and largest orbital momentum values only. It is this last term which breaks the perfect symmetry of the energy formula. It reflects the ordering of the orbitals which do not have periodic boundary conditions. The first and the last orbital are those with the smallest (largest) momentum and can clearly by identified. The first and last orbital do interact but the coupling is different.

3.3.5 Thermodynamics

We have seen the semionic spinon exclusion statistics in Sec. 3.3.3, Eq. (3.32), and the spinonic interaction in Sec. 3.3.2. With these information an alternative thermodynamic Bethe ansatz can be formulated in terms of spinons. The case of an external magnetic field in z-direction is considered which permits to compare with the spinonic result of Sec. 3.2.2. The calculation is entirely performed in the thermodynamic limit. We therefore proceed from the discrete spinon distributions to continuous densities $\rho_\sigma(k)$, one for spin-up ($\sigma=+$) and spin-down ($\sigma=-$) spinons each. The total number of spinons can be expressed by integrals over these spinon densities,

$$n_s = \sum_{\sigma\in\{+,-\}} n_\sigma = \sum_\sigma \int_{k^\sigma_{\min}}^{k^\sigma_{\max}} \frac{\mathrm{d}k}{2\pi}\,\rho_\sigma(k). \tag{3.45}$$

The limits of integration are given by the thermodynamic limit of Eq. (3.31),

$$k^\sigma_{\min} = -\sigma\pi m_z, \qquad k^\sigma_{\max} = \pi(1+\sigma m_z), \tag{3.46}$$

and contain the magnetization (3.26), which can itself be written as integrals over the spinon densities,

$$m_z = \frac{1}{2}\sum_\sigma \sigma n_\sigma = \frac{1}{2}\sum_\sigma \sigma \int_{k^\sigma_{\min}}^{k^\sigma_{\max}} \frac{\mathrm{d}k}{2\pi}\,\rho_\sigma(k). \tag{3.47}$$

We will use the grand canonical picture where the Gibbs free energy is the appropriate thermodynamic potential. It is defined by

$$G = U - TS + PV \tag{3.48}$$

in standard thermodynamics [36]. In lattice models the volume is replaced by the magnetization. The associated parameter is the external magnetic field and the Gibbs free energy $G(T,h)$ depends on the temperature $T=1/(k_B\beta)$ and the external magnetic field h. The equilibrium state is the state of minimum G. We divide by N and write down the Gibbs free energy per site,

$$g(T,h) = u - Ts - hm_z. \tag{3.49}$$

The entropy per site s and the internal energy per site u can be expressed as functions of the spinon densities. Eq. (3.22) leads to the inner energy

$$u = \sum_\sigma \int_{k^\sigma_{\min}}^{k^\sigma_{\max}} \frac{\mathrm{d}k}{2\pi}\,\rho_\sigma(k)\sin k - \frac{1}{\pi}\cos(\pi m_z). \tag{3.50}$$

The entropy can be obtained in the usual way from the distribution of momenta. We use the Bethe ansatz momenta (see Sec. 3.3.3) which are equidistant on a fixed interval. The entropy per site is then found to be

$$s = -k_B \sum_\sigma \int_{k^\sigma_{\min}}^{k^\sigma_{\max}} \frac{\mathrm{d}k}{2\pi} \Big[\rho_\sigma(k) \ln \rho_\sigma(k) + \big(1-\rho_\sigma(k)\big) \ln\big(1-\rho_\sigma(k)\big) \Big]. \tag{3.51}$$

With these ingredients the Gibbs free energy becomes

$$\begin{aligned} g(T,h) &= \sum_\sigma \int_{-\sigma\pi m_z}^{\pi(1+\sigma m_z)} \frac{\mathrm{d}k}{2\pi} \Big\{ \rho_\sigma(k) \sin k + k_B T \Big[\rho_\sigma(k) \ln \rho_\sigma(k) \\ &\quad + \big(1-\rho_\sigma(k)\big) \ln\big(1-\rho_\sigma(k)\big) \Big] - \frac{h}{2} \sigma \rho_\sigma(k) \Big\} - \frac{1}{\pi} \cos(\pi m_z). \end{aligned} \tag{3.52}$$

The equilibrium spinon density must minimize this expression. But we cannot solve the minimization problem directly since the densities are not only in the integrand but also hidden in the limits of integration via (3.47). A way out is suggested by the observation that the integration limits of $\rho_+(k)$ and $\rho_-(k-\pi)$ are complements of the Brillouin zone $[-\pi,\pi]$. We therefore extend the domains (3.46) of the two functions $\rho_+(k)$ and $\rho_-(k)$ via the relation

$$\rho_+(k) + \rho_-(k-\pi) = 1 \tag{3.53}$$

to the full first Brillouin zone and write the Gibbs free energy as integrals over the complete Brillouin zone,

$$\begin{aligned} g(T,h) &= \sum_\sigma \frac{1}{4\pi} \int_{-\pi}^{+\pi} \mathrm{d}k \Big\{ \rho_\sigma(k) \sin k + k_B T \Big[\rho_\sigma(k) \ln \rho_\sigma(k) \\ &\quad + \Big(1-\rho_\sigma(k)\Big) \ln\Big(1-\rho_\sigma(k)\Big) \Big] - h\sigma \rho_\sigma(k) \Big\}. \end{aligned} \tag{3.54}$$

This calculation and the solution of the following variational problem is outlined in Appendix E. The result is the spinon density

$$\rho_\sigma(k) = \Big[e^{\beta(\sin k - h\sigma)} + 1 \Big]^{-1} \tag{3.55}$$

at temperature $T = 1/(k_B\beta)$ and in the external magnetic field h. Thus the equilibrium Gibbs free energy becomes

$$g_{\mathrm{eq}}(\beta,h) = -k_B T \int_{-\pi}^{+\pi} \frac{\mathrm{d}k}{2\pi} \ln\Big(2\cosh \frac{\beta}{2}(h+\sin k) \Big). \tag{3.56}$$

This result has been previously obtained in the fermionic picture by Katsura [35], see (3.16). At this point we have shown that the thermodynamics of the XX model can be described entirely in the formalism of spinons since all interesting thermodynamic quantities can be derived from the Gibbs free energy.

3.4 The Dynamic Spin Structure Factor $S_{-+}(q,\omega)_0$

In connection with Sec. 2.4 we will analyze the dynamic spin structure factor $S_{-+}(q,\omega)_0$ for the XX model. It is one of the structure factors given in (2.59) where the index zero indicates that only transitions from the ground state are considered. In the degenerate case of odd N transitions from all ground states are calculated.

3.4.1 Circumnavigating Critical Pairs

The crucial part of the dynamic spin structure factors are the transition rates (see Sec. 2.4). Here we will give the transition rates $M_\lambda^\pm$ from Eq. (2.49) for the XX case explicitely. The calculation of the limit $\Delta \to 0$ is sketched in [18] yielding

$$M_\lambda^+(q) = \frac{\prod_{i<j}^{r+1} \sin^2 \frac{k_i - k_j}{2} \prod_{i<j}^{r} \sin^2 \frac{k_i^0 - k_j^0}{2}}{N^{2r} \prod_{i=1}^{r} \prod_{j=1}^{r+1} \sin^2 \frac{k_i^0 - k_j}{2}} \tag{3.57}$$

$$M_\lambda^-(q) = \frac{\prod_{i<j}^{r-1} \sin^2 \frac{k_i - k_j}{2} \prod_{i<j}^{r} \sin^2 \frac{k_i^0 - k_j^0}{2}}{N^{2r-2} \prod_{i=1}^{r} \prod_{j=1}^{r-1} \sin^2 \frac{k_i^0 - k_j}{2}} \tag{3.58}$$

where the sets $\{k_i^0, i = 1, \ldots, r\}$ and $\{k_i, i = 1, \ldots, r \pm 1\}$ are magnon momenta, that is, solutions of the XX limit of the Bethe ansatz equations (2.22). To be precise, the set $\{k_i^0\}$ describes the ground state $|\psi_0\rangle$ of the system in the notation of (2.48) and the set $\{k_i\}$ belongs to the excited state $|\psi_\lambda\rangle$. Originally, the results (3.57) and (3.58) were proven in [18] only under the restriction that among the magnon momenta there is no pair k_i, k_j with the property $k_i + k_j = (\pi \mod 2\pi)$ present. Those *critical pairs* cannot occur in the ground state but are present in some excitations. The reason for this exclusion is that the limit $\Delta \to 0$ leads to undetermined expressions in (2.49) for critical pairs since the determinant $\det \mathsf{H}$ vanishes and the prefactor diverges. But it turns out that in the end all problematic factors cancel out, leaving us with the highly compact results (3.57) and (3.58).
So the idea arose that these results might be valid even for those excitations with critical pairs. Checks for small systems showed, however, that substituting the critical magnon momenta yields wrong results. A way out has finally been found in [34]. Our idea bases on the observation that the set of magnon momenta is always identical with the set of fermion momenta as long as no critical pairs are present. And if there are some, all noncritical magnon momenta are still identical with their fermionic counterparts. But the additional fermionic momenta are different from all critical and noncritical magnon momenta. So one is naturally led to the conjecture that the formulas (3.57) and (3.58) are indeed valid for all excitations if only the magnon momenta are replaced by their fermionic counterparts.
The conjecture has been tested numerically. The obtained matrix elements fulfill the sum rule

$$\sum_q \left[\sum_{n'} M_{nn'}^+(q) + \sum_{n''} M_{nn''}^-(q) \right] = N \qquad \forall n \tag{3.59}$$

for both even and odd values of the system size N up to 24. The fixed state $|n\rangle$ was chosen as the unique ground state for even N. In the case of odd N the sum rule was tested individually for each degenerate ground state for $|n\rangle$.
In [18] we failed to proof (3.57) and (3.58) in the magnon picture for generic states because of overwhelming technical problems with critical pairs. It might be possible to work out an independent proof in the fermion picture but we did not follow that line any further.

3.4.2 Transitions from the Ground State for Even N

We have restricted our numerical studies to transitions from the ground state. Experimentally speaking this restriction implies that the system is at zero temperature, $T = 0$. For even N the ground state

is the unique spinon vacuum. The corresponding fermion configuration is depicted in the first row of Fig. 6 for $N = 12$. The ground state contains $N/2$ fermions with momenta $\{k_i^0\}$. The vertical lines in the picture separate the inside and outside marked by the $\vee$-shaped line in Fig. 1(a).

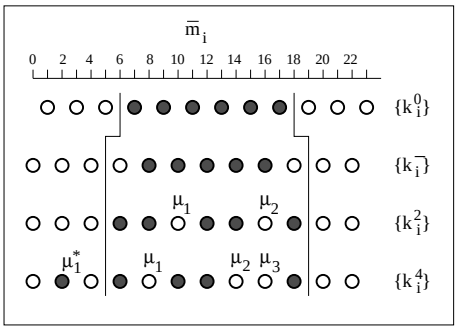

Figure 6: System with $N = 12$ sites. Fermion momenta $k_i = (\pi/N)\bar{m}_i$ for the lowest energy states at $N_f = N/2$ (row 1) and $N_f = N/2 - 1$ (row 2). Also shown are the fermion momenta for a generic 2-spinon state (row 3) and a generic 4-spinon state in the subspace with $N_f = N/2 - 1$. Also shown are segments of the two-pronged fork described in the context of Fig. 3

It is necessary to generate the excitations in a systematic way. Therefore we start with the ground state in the invariant subspace sketched in the second row of Fig. 6. It contains $N_f = N/2-1$ fermions with momenta $\{k_i^-\}$.
All excitations contain an even number of spinons. The excitations of two spinons are generated by moving the two vacancies through the inside. An example is given in the third row of Fig. 6. Apparently the 2-spinon excitations can be parameterized by the two even-valued numbers $N/2 \leq \mu_1 < \mu_2 \leq 3N/2$ which mark the vacancies' positions in the array of the fermion momenta $\{k_i^2\}$. They represent two spinons with spin up and momenta as given by the rules in Sec. 3.3.
The excitations of more than two spinons are generated by moving fermions from the inside to the outside. With every moved fermion two spinons are created, one up-spinon in the inside and one down-spinon in the outside. The excitations of four spinons are thus described by four even parameters $\mu_1, \mu_2, \mu_3, \mu_1^*$, where $N/2 \leq \mu_1 < \mu_2 < \mu_3 \leq 3N/2$ are the positions of the vacancies and μ_1^* either in the range $0 \leq \mu_1^* < N/2$ or $3N/2 < \mu_1^* < 2N$ is the position of the outside fermion. Thus a $2m$-spinon state contains $n_+ = m + 1$ up-spinons and $n_- = m - 1$ down-spinons.
The parameters μ_i and μ_i^* can be related to the change of energy and momentum during the transition. Once the spinon momenta of a state n are known the total wave number is simply given by the sum of all spinon momenta,

$$k_T^n = \sum_i k_i^n \mod 2\pi \tag{3.60}$$

and hence the change of wave number during the transition from n to n' is

$$q = \Big(\sum_i k_i^n - \sum_i k_i^{n'} \Big) \mod 2\pi. \tag{3.61}$$

The simultaneous energy transfer is

$$\omega = \sum_i \cos(k_i^{n'}) - \sum_i \cos(k_i^n). \tag{3.62}$$

3.4.3 The Total m-Spinon Intensity for Even N

The dynamical structure factor $S_{-+}(q,\omega)_0$ is built up by the contributions of all spinon excitations. Bearing in mind the parameterization of the classes of spinon excitations given in Sec. 3.4.2 it is natural to calculate the contribution of these classes to $S_{-+}(q,\omega)_0$ separately. We perform these calculations for the excitation of two and four spinons for reasonably large systems so that the behaviour in the limit $N \to \infty$ can be extrapolated. For both classes we give the relative part I_m/I_{tot} where

$$I_{\mathrm{tot}} = \sum_q \sum_n M^-_{0n}(q) = \sum_{m=2,4,\ldots} I_m = \frac{N}{2} \tag{3.63}$$

is the integrated total of the static structure factor.

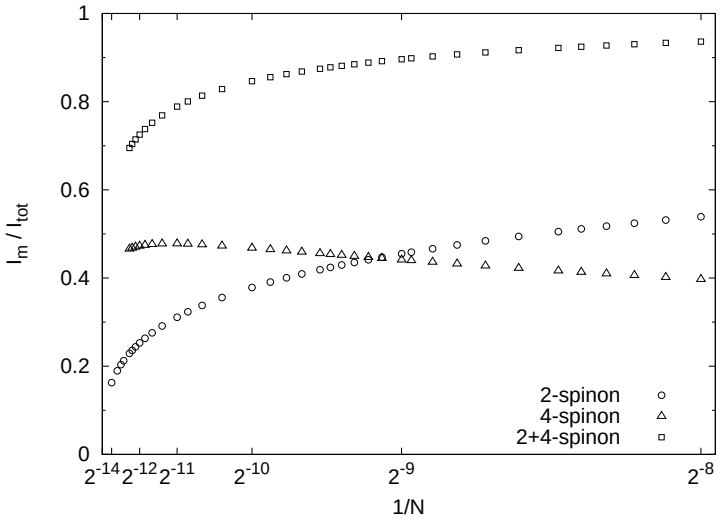

Figure 7: Relative overall intensity of the 2-spinon excitations and 4-spinon excitations in $S_{-+}(q,\omega)_0$ plotted versus $1/N$. The squares denote the sum of both excitations.

The numeric results are given in Fig. 7. They yield two-fold information:

- On the one hand, the total intensity for $m = 2$ evidently drops to zero in the limit $N \to \infty$. The calculation was performed for N up to 2^{14} and the numeric indication is doubtless. The same seems to hold for $m = 4$ although the extrapolation is difficult in that case due to the much smaller number of data points $N \lesssim 2^{12}$. The turning point is clearly visible with a maximum around 2^{11} but we do not have many data points beyond the maximum. Nevertheless we do expect that any m-spinon contribution taken individually will vanish in that limit. Hence we cannot obtain any information about the infinite chain from any finite size data this way.
- On the other hand, we see that the combined 2-spinon and 4-spinon relative intensity stays above 80% for chains with up to $N \simeq 2000$ sites. This information is surely important for experiments where system sizes of only several hundred or a few thousand sites are quite common.

3.4.4 Asymptotic Transition Rates for Even N

The data of Fig. 7 have been obtained from the product formula (3.58). In this section we demonstrate how these products can be expanded asymptotically for $N \to \infty$. For reasons of technical convenience

we have factorized the huge product expression into (i) one factor which is the same for every class of excitations (the *scaling factor*) and (ii) the remainders (the *scaled transition rate*) which contain the excitation:

$$M^-\big(\{k_i^0\},\{k_i^m\}\big) = \underbrace{\frac{M^-\big(\{k_i^0\},\{k_i^m\}\big)}{M^-\big(\{k_i^0\},\{k_i^-\}\big)}}_{\text{scaled transition rate}} \times \underbrace{M^-\big(\{k_i^0\},\{k_i^-\}\big)}_{\text{scaling factor}}. \tag{3.64}$$

The sets $\{k_i^0\}$ and $\{k_i^-\}$ are the fermion momenta of the ground states in the invariant Hilbert subspaces with $N_f = N/2$ and $N_f = N/2-1$, respectively. Together with the fermion momenta $\{k_i^m\}$ of the excitation they are sketched in Fig. 6 for $m = 2, 4$.
The scaling factor can be brought into the compact form

$$M^-\big(\{k_i^0\},\{k_i^-\}\big) = \sqrt{N} \times C_N(N/2), \tag{3.65}$$

$$C_N(n) = \prod_{l=1}^{n} \frac{\sin^{4l-3}\eta(l-1/2)}{\sin^{4l-1}\eta l}, \qquad \eta = \frac{\pi}{N}, \tag{3.66}$$

and tends towards a constant

$$C = \lim_{N\to\infty} C_N(N/2) = \sqrt{\pi}\exp\Big(\frac{\ln 2}{6} + \zeta'(-1)\Big) = 0.737\,390\,711\,766\,\ldots \tag{3.67}$$

in the thermodynamic limit as is shown in App. A.

3.4.5 Asymptotic 2-Spinon Transition Rates

The scaled transition rate for a 2-spinon excitation can be written explicitly for any specific excitation by simply putting the concrete spinon momenta into the product formulas (3.57) and (3.58). Most of the factors cancel since the two states differ by not more then two momenta. The calculation is technically simple but nevertheless laborious since the exceptional cases $\mu_1 = N/2$ and $\mu_2 = 3N/2$ must be treated separately. We introduce the shifted and scaled parameters

$$\psi_i = \frac{\mu_i}{2} - \frac{N}{4} \qquad \text{and} \qquad \kappa_i = \frac{\pi}{N}\mu_i, \qquad i = 1,2 \tag{3.68}$$

in which the scaled matrix element reads

$$\begin{aligned} &\frac{M^-\big(\{k_i^0\},\{k_i^2\}\big)}{M^-\big(\{k_i^0\},\{k_i^-\}\big)} \\ &= \left(\prod_{l=1}^{N/2} \frac{\sin^2\left(\frac{\pi l}{N}\right)}{\sin\left(\frac{\pi l}{N}-\frac{\pi}{2N}\right)\sin\left(\frac{\pi l}{N}+\frac{\pi}{2N}\right)}\right)^2 \left(\prod_{j=1}^{2}\prod_{\substack{l=1\\ l\neq\psi_j}}^{N/2} \frac{\sin\left(\frac{\pi}{N}(l-\psi_j)-\frac{\pi}{2N}\right)}{\sin\left(\frac{\pi}{N}(l-\psi_j)\right)}\right)^2 \\ &\sin^2\left(\frac{\pi}{2N}\right)\cos^2\left(\frac{\pi}{2N}\right)\underbrace{\sin^{-2}\left(\frac{\kappa_1}{2}-\frac{\pi}{4}\right)}_{\text{if } \mu_1\neq N/2}\sin^{-2}\left(\frac{\kappa_2}{2}-\frac{\pi}{4}\right)\sin^2\left(\frac{\kappa_1-\kappa_2}{2}\right)\underbrace{\sin^{-2}\left(\frac{\pi}{2N}\right)}_{\text{if } \mu_1=N/2}. \end{aligned} \tag{3.69}$$

The underbraced factors are present only if the underset condition is fulfilled. We hope that no confusion between the parameter κ_i in (3.68) and the spinon momenta κ_i in Eq. (3.17) arises.

The two products in the second line are of similar structure and can therefore be written as special values of the same function. This function can be chosen such that it absorbs most of the prefactors and also the conditional expressions,

$$\frac{M^-\big(\{k_i^0\},\{k_i^2\}\big)}{M^-\big(\{k_i^0\},\{k_i^-\}\big)} = N^2 \sin^2\frac{\kappa_1-\kappa_2}{2}\prod_{j=1}^{2}\phi(\psi_j)\phi(N/2-\psi_j) \tag{3.70}$$

where the function ϕ is defined by

$$\phi(n) = \prod_{l=1}^{n}\frac{\sin^2\eta(l-\frac{1}{2})}{\sin^2\eta l} \quad \text{for} \quad n\in\mathbb{N}^+ \quad \text{with} \quad \phi(0)=1. \tag{3.71}$$

Again we have set $\eta=\pi/N$. It is the definition of $\phi(0)$ which reproduces the conditionals in (3.69). The remaining ϕ-functions can be expanded asymptotically for large N. During the calculation it turns out that the scaled matrix element diverges at the boundaries $\mu_1 = N/2 \Leftrightarrow \psi_i = 0$ and $\mu_2 = 3N/2 \Leftrightarrow \psi_2 = N/2$. Thence we restrict the expansion to the range $m<\psi_1<\psi_2<N/2-m$ which only asymptotically becomes the full spectrum. The threshold is chosen to be

$$m = \big[\sqrt{N}\,\big] \tag{3.72}$$

where $[\ldots]$ denotes the integer part. In App. B we derive the asymptotic expansion

$$\phi(n) = \frac{1}{N\sin\frac{n\pi}{N}}\times\big[1+\mathcal{O}\left(1/N\right)\big] \tag{3.73}$$

for not too small arguments $n \gtrsim \mathcal{O}\left(m\right)$. Hence the expansion of the scaled matrix element is

$$\frac{M^-\big(\{k_i^0\},\{k_i^2\}\big)}{M^-\big(\{k_i^0\},\{k_i^-\}\big)} = \frac{\sin\frac{\kappa_1-\kappa_2}{2}\big[1+\mathcal{O}\left(1/N\right)\big]}{N^2\prod_{j=1}^{2}\sin\left(\frac{\pi\psi_i}{N}\right)\sin\left(\frac{\pi}{2}-\frac{\pi\psi_i}{N}\right)} = \frac{1}{N^2}\,\frac{\sin\frac{\kappa_1-\kappa_2}{2}}{\cos\kappa_1\cos\kappa_2}\times\big[1+\mathcal{O}\left(1/N\right)\big] \tag{3.74}$$

where we have used (3.68) to transform the ψ's into κ's. The constraint of not too small momenta κ_i is due to the mentioned singularity along the spectral border.
The spinon momenta κ_1 and κ_2 can be translated into the physically more interesting exchange of energy ω and wave number q via Eqs. (3.61) and (3.62). Substituting the specific spinon states immediately yields

$$q = \left(\pi-\kappa_1-\kappa_2\right) \mod 2\pi \tag{3.75}$$

$$\omega = -\cos\kappa_1-\cos\kappa_2+\sum_{l=1}^{N/2}\left[\sin\left(\frac{2\pi l}{N}-\frac{\pi}{N}\right)-\sin\left(\frac{2\pi l}{N}\right)\right] \tag{3.76}$$

where

$$\sum_{l=1}^{N/2}\left[\sin\left(\frac{2\pi l}{N}-\frac{\pi}{N}\right)-\sin\left(\frac{2\pi l}{N}\right)\right] = \frac{1-\cos\frac{\pi}{N}}{\sin\frac{\pi}{N}} = -\frac{\pi}{2N}+\mathcal{O}\left(N^{-3}\right). \tag{3.77}$$

The first equality is elementary proven by the use of certain summation formulas for the sine and cosine [40],

$$\sum_{l=0}^{N/2} \sin\Big(\frac{2\pi l}{N}\Big) = \cot\Big(\frac{\pi}{N}\Big), \qquad \sum_{l=0}^{N/2} \cos\Big(\frac{2\pi l}{N}\Big) = 0. \tag{3.78}$$

In the variables q and ω the asymptotic 2-spinon transition rate (3.64) reads

$$M_2^-(q,\omega) \stackrel{a}{=} \frac{4C}{N^{3/2}} \, \frac{4\sin^2(q/2) - \omega^2}{\omega^2 - \sin^2 q}. \tag{3.79}$$

It is defined on the first Brillouin zone $0 \le q \le 2\pi$. Here and in the following the symbol "$\stackrel{a}{=}$" denotes asymptotic equality in the thermodyamic limit $N \to \infty$. The energy transfer is asymptotically bounded by

$$|\sin(q)| \;\le\; \omega \;\le\; 2|\sin(q/2)|. \tag{3.80}$$

Multiplying the transition rate with the density of states yields the dynamical structure factor. For the excitation of two spinons the asymptotic density function is well known to be [41]

$$D_2(q,\omega) \stackrel{a}{=} \frac{N}{2\pi} \, \frac{1}{\sqrt{4\sin^2(q/2) - \omega^2}} \tag{3.81}$$

and thus the asymptotic 2-spinon part of the dynamical structure factor for transitions from the ground state is found to be

$$S^{(2)}_{-+}(q,\omega)_0 \stackrel{a}{=} \frac{2C}{\pi\sqrt{N}} \, \frac{\sqrt{4\sin^2(q/2) - \omega^2}}{\omega^2 - \sin^2 q} \tag{3.82}$$

where the constant C has been given in (3.67). This result requires some comments:

- Since equality is only asymptotic large values of N are required to suppress the corrections. Thus the larger N the clearer the shape of the function becomes.
- But on the other hand the right hand side clearly vanishes in the thermodynamic limit and the approximate result becomes exact only the moment it disappears.
- That means that the 2-spinon excitation does not contribute to the dynamic structure factor of the infinite system at all. But that was, of course, already predicted by numerical studies shown in Fig. 7.

3.4.6 Asymptotic 4-Spinon Transition Rates

Again we start with the factorization (3.64). The required spinon momenta have already been encoded in Fig. 6. Proceeding along similiar lines as in the case of two spinons we substitute the spinon momenta, perform massive cancellations, and write the result in terms of scaled momenta:

$$\begin{aligned} \frac{M^-\big(\{k_i^0\},\{k_i^4\}\big)}{M^-\big(\{k_i^0\},\{k_i^-\}\big)} \;&=\; N^2 \sin^2\left(\frac{\kappa_1^*}{2} - \frac{\pi}{4}\right) \frac{\displaystyle\prod_{i<j}^{3} \sin^2 \frac{\kappa_i - \kappa_j}{2}}{\displaystyle\prod_{i=1}^{3} \sin^2 \frac{\kappa_1^* - \kappa_i}{2}} \\ &\quad \times \frac{\phi(N/4 - \mu_1^*/2)}{\phi(3N/4 - \mu_1^*/2)} \prod_{j=1}^{3} \phi(\psi_j)\phi(N/2 - \psi_j) \end{aligned} \tag{3.83}$$

where

$$\psi_i = \frac{\mu_i}{2} - \frac{N}{4}, \quad \kappa_i = \eta\mu_i, \quad i = 1,2,3, \qquad \kappa_1^* = \eta\mu_1^* \tag{3.84}$$

and the function ϕ is the same as in Eq. (3.71). Using expansion (B.6) of the ϕ-function the asymptotic expansion

$$\frac{M^-\big(\{k_i^0\},\{k_i^4\}\big)}{M^-\big(\{k_i^0\},\{k_i^-\}\big)} = \frac{4}{N^4} \times \frac{\cos(\kappa_1^*)}{\prod_{i=1}^{3}\cos(\kappa_i)} \times \frac{\prod_{i<j}^{3}\sin^2\frac{\kappa_i-\kappa_j}{2}}{\prod_{i=1}^{3}\sin^2\frac{\kappa_1^*-\kappa_i}{2}} \tag{3.85}$$

for the scaled 4-spinon transition rate is obtained. It depends on the energy and momentum transfer via Eqs. (3.61) and (3.62) which in this case specialize to

$$\omega \stackrel{a}{=} \cos\kappa_1^* - \sum_{i=1}^{3}\cos\kappa_i, \qquad q = \pi + \kappa_1^* - \sum_{i=1}^{3}\kappa_i \bmod 2\pi. \tag{3.86}$$

Unlike the 2-spinon case, it is no more possible to invert these equations. Therefore we cannot write the dependency of $M_4^-(q,\omega)$ on q and ω explicitly. But what we still can get is the spectral range in the $(q-\omega)$-plane which is illustrated in Fig. 8. The 4-spinon excitation shares the spectral threshold

$$\epsilon_{2L}(q) = \epsilon_{4L}(q) = |\sin q| \tag{3.87}$$

with the 2-spinon excitation, but it has a different upper boundary,

$$\epsilon_{2U}(q) = 2\left|\sin\frac{q}{2}\right|, \tag{3.88}$$

$$\epsilon_{4U}(q) = 4\max\left[\left|\sin\frac{q}{4}\right|, \left|\sin\frac{q-2\pi}{4}\right|\right]. \tag{3.89}$$

The distribution of circles reveals the nonuniform density of 2-spinon states which is large along the upper spectral border and small near the soft mode $q \simeq \pi$, $\omega \simeq 0$. The density of 4-spinon states is encoded in the dots. It is comparatively small below $\omega \lesssim 1$ and large near the upper spectral border.

3.4.7 Transitions from the Ground State for Odd N

For odd N the ground state is fourfold degenerate and contains $(N\pm1)/2$ fermions. We label the two ground state configurations with $N_f = (N-1)/2$ by A and A' and the other two configurations by B and B'. The corresponding spinon momenta are sketched in Fig. 9 for $N = 11$ sites.
The ground states A' and B' have the spinon momenta of the ground states A and B reflected at the middle of the Brillouin zone ($m_i = N$). Thus the transition rates by symmetry are the same with negative momentum exchange, $S_{\mu\nu}(q,\omega)_{A'} = S_{\mu\nu}(-q,\omega)_A$ and $S_{\mu\nu}(q,\omega)_{B'} = S_{\mu\nu}(-q,\omega)_B$. Since each ground state contributes to the dynamic spin structure factor we have to deal with the average

$$S_{\mu\nu}(q,\omega) = \frac{1}{4}\left[S_{\mu\nu}(q,\omega)_A + S_{\mu\nu}(-q,\omega)_A + S_{\mu\nu}(q,\omega)_B + S_{\mu\nu}(-q,\omega)_B\right]. \tag{3.90}$$

The accessible excitations contain only odd spinon numbers. The ground state A contains $(N-1)/2$ fermions and the accessible excitations contain even less fermions, thus at least three spinons as is

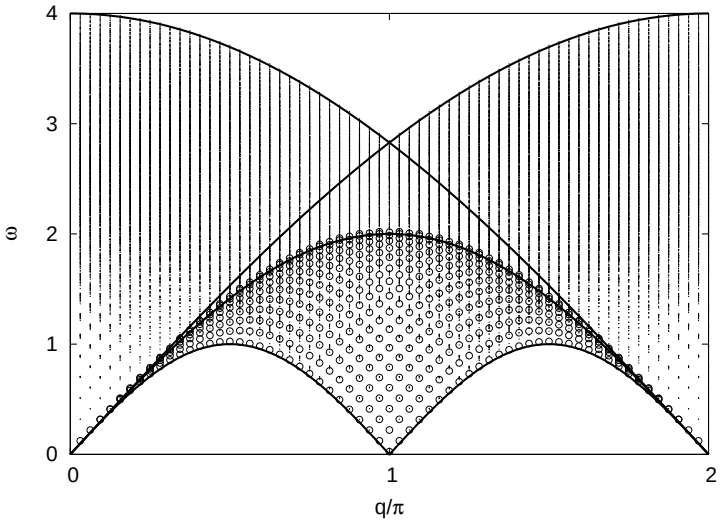

Figure 8: Excitation energy versus wave number of all 2-spinon ($\circ$) and 4-spinon ($\cdot$) excitations for $N = 64$. The solid lines are the spectral boundaries (3.87), (3.88), and (3.89) for $N \to \infty$.

sketched in the third row of Fig. 9. But the ground state B contains $(N+1)/2$ fermions so that excitations with only one spinon can be reached. Typical excitations of one and three spinons are sketched in the sixth and seventh row of Fig. 9. The accessible 3-spinon states are not the same for both ground states, but state A accesses states with three up-spinons, whereas transitions from state B lead to states with two up-spinons and one down-spinon. Therefore the three-spinon part of the dynamical spin structure factor must be calculated separetely for both ground states.
We follow the analysis of even N (see Sec. 3.4.3) and introduce relative intensities. This time, we define the relative one spinon intensity $I_1^B/I_{\rm tot}$ and the relative two spinon intensities $I_3^A/I_{\rm tot}^A$ and $I_3^B/I_{\rm tot}^B$, where

$$\begin{aligned} I_{\rm tot}^A &= \sum_q \sum_n M_{An}^-(q) = \sum_{m=3,5,\ldots} I_m^A = \frac{N-1}{2}, \\ I_{\rm tot}^B &= \sum_q \sum_n M_{Bn}^-(q) = \sum_{m=1,3,\ldots} I_m^B = \frac{N+1}{2}. \end{aligned} \tag{3.91}$$

The relative intensities for one and three spinons are calculated numerically for chains with up to $N = 2^{16} - 1$ for I_1^B and $N = 2^{12} - 1$ for I_3^A and I_3^B. We give these finite-N data in Fig. 10. The observations are qualitatively the same as in the case of even N: On the one hand, the combined intensities of one and three spinons are relevant for chains with some hundred to some thousand sites and stay above 50% for $N \lesssim 1500$. But on the other hand, all three relative intensities do each drop to zero in the thermodynamic limit.

3.4.8 Asymptotic Transition Rates for Odd N

We follow Sec. 3.4.4 and again separate the transition function into the scaled transition function and a scaling factor. But this time we need two different scaling factors, one for each ground state.

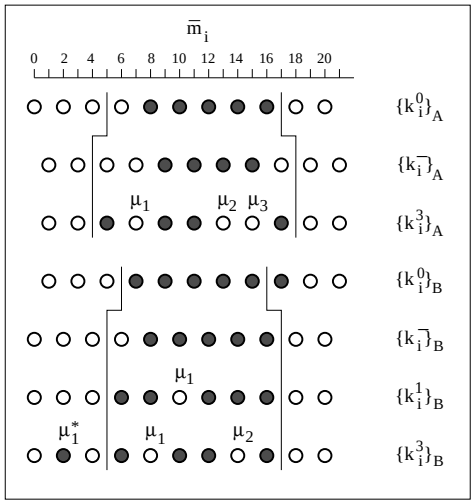

Figure 9: XX chain with $N = 11$ sites. Fermion momenta $k_i = (\pi/N)\bar{m}_i$ for one of two lowest energy states at $N_f = (N-1)/2$ (rows 1 and 5), $N_f = (N-3)/2$ (row 2), and $N_f = (N+1)/2$ (row 4). The other state in each case (henceforth referred to by subscripts A' or B') is obtained via reflection at the line $\bar{m}_i = 11$. Also shown are the fermion momenta for a generic 1-spinon state in the subspace with $N_f = (N-1)/2$ (row 6), a generic 3-spinon state in the subspace with $N_f = (N-3)/2$ (row 3), and a generic 3-spinon state in the subspace with $N_f = (N-1)/2$ (row 7).

Fortunately, both can be written in terms of the function $C_N(n)$ from equation (3.66) which appears with a slightly shifted argument this time. The two scaling factors are

$$M^-\big(\{k_i^0\}_A, \{k_i^-\}_A\big) = \sqrt{N}\, C_N((N-1)/2)\, \cos^2\frac{\eta}{2}, \tag{3.92}$$

$$M^-\big(\{k_i^0\}_B, \{k_i^-\}_B\big) = \sqrt{N}\, C_N((N-1)/2), \tag{3.93}$$

which asymptotically approach the same value,

$$M^-\big(\{k_i^0\}_A, \{k_i^-\}_A\big) \stackrel{a}{=} M^-\big(\{k_i^0\}_B, \{k_i^-\}_B\big) \stackrel{a}{=} \sqrt{N}\, C \tag{3.94}$$

with the constant C from (3.67). The scaled transition rate function for 1-spinon excitations can again be written as a product of ϕ-functions,

$$\frac{M^-\big(\{k_i^0\}_B, \{k_i^1\}_B\big)}{M^-\big(\{k_i^0\}_B, \{k_i^-\}_B\big)} = N\cos^2(\eta\psi_1)\phi(\psi_1)\phi((N-1)/2-\psi_1), \tag{3.95}$$

where

$$\psi_1 = \frac{\mu_1}{2} - \frac{N+1}{4}, \quad \kappa_1 = \eta\mu_1, \quad \eta = \frac{\pi}{N} \tag{3.96}$$

and the function ϕ is the same as in Eq. (3.71). Using the known asymptotic of the ϕ-functions (see App. B), we derive the asymptotic result

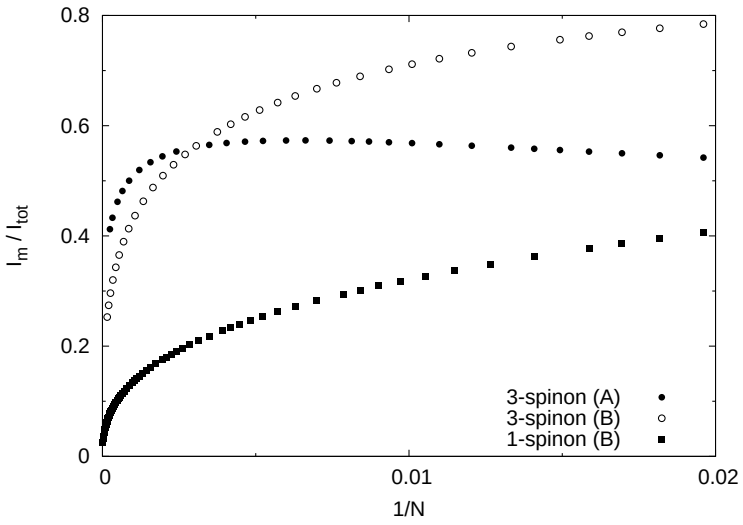

Figure 10: Relative overall intensity of the 1-spinon excitations (■) and 3-spinon excitations (○) in $S_{-+}(q,\omega)_B$, and of the 3-spinon excitations (●) in $S_{-+}(q,\omega)_A$, all plotted versus $1/N$.

$$\frac{M^-\big(\{k_i^0\}_B,\{k_i^1\}_B\big)}{M^-\big(\{k_i^0\}_B,\{k_i^-\}_B\big)} \stackrel{a}{=} \frac{1}{N}\cot\Big(\frac{\kappa_1}{2}-\frac{\pi}{4}\Big)\,. \tag{3.97}$$

From Eqs. (3.61) and (3.62) it is possible to express the spinon momentum κ_1 by the exchange of energy and wave number,

$$\omega \stackrel{a}{=} -\cos\kappa_1, \qquad q \stackrel{a}{=} \frac{3\pi}{2}-\kappa_1. \tag{3.98}$$

The transition rate function

$$M_1^-(q,\omega)_B \stackrel{a}{=} C\,N^{-1/2}\,\tan\frac{q}{2} \tag{3.99}$$

is independent of ω on the whole spectrum $0 \le \omega \le 1$. The excitation of a single spinon is, of course, an isolated branch in the spectrum and thus the density of states reduces to a delta function. Multiplying it with the transition rate function yields the 1-spinon part of the asymptotic dynamical spin structure factor,

$$S_{-+}^{(1)}(q,\omega) \stackrel{a}{=} \frac{C}{4\sqrt{N}}\,\tan\frac{q}{2}\,\delta\left(\omega-|\sin q|\right), \tag{3.100}$$

where the factor $1/4$ incorporates the ground state's four-fold degeneracy.
For the 3-spinon excitation we must do the calculation twice, one for each ground state. The scaled transition rate function for ground state B is found to be

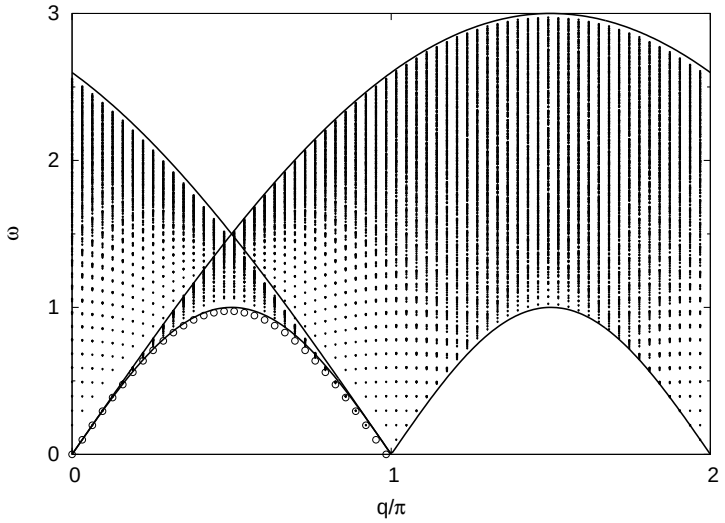

Figure 11: Excitation energy versus wave number of all 1-spinon excitations ($\circ$) and 3-spinon excitations ($\cdot$) from ground-state B for $N = 63$. The solid lines are the 3-spinon continuum boundaries for $N \to \infty$. The corresponding 1-spinon and 3-spinon spectrum from ground-state B' is the mirror image reflected at $q/\pi = 1$ of the spectrum shown.

$$\begin{aligned}\frac{M^-\big(\{k_i^0\}_B,\{k_i^3\}_B\big)}{M^-\big(\{k_i^0\}_B,\{k_i^-\}_B\big)} &= N\tan^2(\eta\psi_1^*)\sin^2(\eta(\psi_1-\psi_2))\prod_{j=1}^{2}\frac{\cos^2(\eta\psi_j)}{\sin^2(\eta(\psi_1^*-\psi_j))} \\ &\quad\times\frac{\phi(-\psi_1^*)}{\phi((N-1)/2-\psi_1^*)}\prod_{j=1}^{2}\phi(\psi_j)\phi((N-1)/2-\psi_j) \qquad (3.101)\end{aligned}$$

and depends on the three parameters

$$\psi_1 = \frac{\mu_1}{2}-\frac{N+1}{4},\quad \psi_2 = \frac{\mu_2}{2}-\frac{N+1}{4},\quad \psi_1^* = \frac{\mu_1^*}{2}-\frac{N+1}{4}. \qquad (3.102)$$

The asymptotic expansion is

$$\frac{M^-\big(\{k_i^0\}_B,\{k_i^3\}_B\big)}{M^-\big(\{k_i^0\}_B,\{k_i^-\}_B\big)} \stackrel{a}{=} \frac{1}{N^3}\,\frac{\sin^2\big(\frac{\kappa_1-\kappa_2}{2}\big)}{\prod_{i=1}^{2}\tan\big(\frac{\kappa_i}{2}-\frac{\pi}{4}\big)}\,\frac{\tan\big(\frac{\pi}{4}-\frac{\kappa_1^*}{2}\big)}{\prod_{i=1}^{2}\sin^2\big(\frac{\kappa_1^*-\kappa_i}{2}\big)}. \qquad (3.103)$$

It depends on the three parameters

$$\kappa_1 = \eta\mu_1, \qquad \kappa_2 = \eta\mu_2, \qquad \kappa_1^* = \eta\mu_1^* \qquad (3.104)$$

being related to the energy and wave number exchange via

$$\omega \stackrel{a}{=} \cos\kappa_1^* - \sum_{i=1}^{2}\cos\kappa_i, \qquad q \stackrel{a}{=} \kappa_1^* - \sum_{i=1}^{2}\kappa_i - \frac{\pi}{2} \mod 2\pi. \qquad (3.105)$$

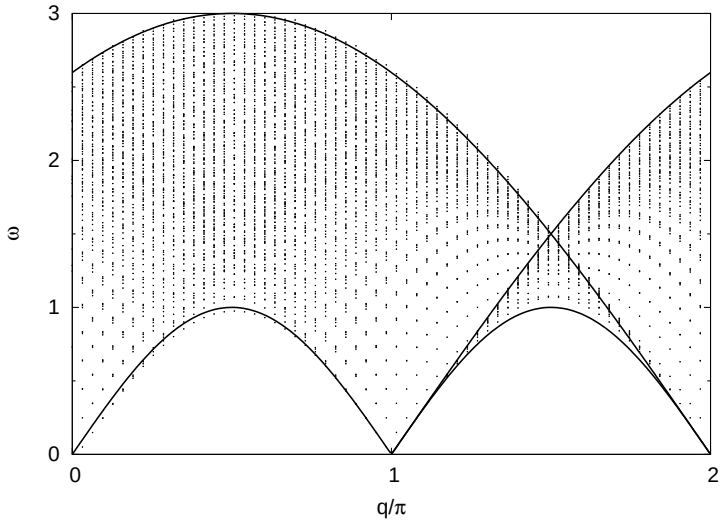

Figure 12: Excitation energy versus wave number of all 3-spinon excitations from ground-state A for $N = 63$. The solid lines are the 3-spinon continuum boundaries for $N \to \infty$. The corresponding 3-spinon spectrum from the ground-state component A' is the mirror image reflected at $q/\pi = 1$ of the spectrum shown.

The range of excitations of one and three spinons from ground state B is shown in Fig. 11 for $N = 63$. The spectrum reached from ground state B' is obtained if the wave number q is replaced by $2\pi - q$. For $N \to \infty$ the single one-spinon branch coincides with the spectral threshold of the three-spinon continuum,

$$\epsilon_1(q) = \epsilon_{3L}(q) = |\sin q|. \tag{3.106}$$

The asymptotic upper boundary of the 3-spinon continuum is

$$\epsilon_{3U}(q) = 3 \max\left(\left|\sin \frac{q}{3}\right|, \left|\sin \frac{q-2\pi}{3}\right| \right). \tag{3.107}$$

These boundaries are shown in Fig. 11 as solid lines. Ground state A leads to excitations of at least three spinons. All accessible 3-spinon states $\{k_i^3\}_A$ have spin 3/2 and are different from the states $\{k_i^3\}_B$ so that the transition rate function must be calculated anew. Again we follow the lines of Sec. 3.4.3 and 3.4.4 and obtain this time the scaled transition rate function

$$\frac{M^-\left(\{k_i^3\}_A, \{k_i^0\}_A\right)}{M^-\left(\{k_i^-\}_A, \{k_i^0\}_A\right)} = N^3 \left(\sin^2 \frac{\eta}{2}\right) \frac{\prod_{i<j}^{3} \sin^2(\eta(\psi_i - \psi_j))}{\prod_{j=1}^{3} \sin^2(\eta(\psi_j - 1/2))} \left(\prod_{j=1}^{3} \phi(\psi_j)\phi((N+1)/2 - \psi_j) \right) \tag{3.108}$$

which depends on the three parameters

$$\psi_i = \frac{\mu_i}{2} - \frac{N-1}{4}, \quad i = 1, 2, 3. \tag{3.109}$$

We write the asymptotic expansion as a function of the scaled variables $\kappa_i = \eta\mu_i$:

$$\frac{M^-\left(\{k_i^3\}_A,\{k_i^0\}_A\right)}{M^-\left(\{k_i^-\}_A,\{k_i^0\}_A\right)} \stackrel{a}{=} \frac{\pi^2}{4N^5} \times \frac{\prod_{i<j}^{3} \sin^2 \frac{\kappa_i-\kappa_j}{2}}{\prod_{i=1}^{3} \cos\left(\frac{\kappa_i}{2}-\frac{\pi}{4}\right) \sin^3\left(\frac{\kappa_i}{2}-\frac{\pi}{4}\right)}. \tag{3.110}$$

From Eqs. (3.61) and (3.62) we obtain the transfer and energy and momentum in these variables,

$$\omega \stackrel{a}{=} -\sum_{i=1}^{3} \cos\kappa_i, \qquad q \stackrel{a}{=} \frac{3\pi}{2} - \sum_{i=1}^{3} \kappa_i \mod 2\pi. \tag{3.111}$$

The range in the (q,ω)-plane of the 3-spinon excitations from ground-state A is shown in Fig. 12 for $N = 63$. The corresponding spectrum reached from ground-state component A' is the one with wave numbers q replaced by $2\pi - q$. In the limit $N \to \infty$ the 3-spinon continuum boundaries for states A and A' combined are the same as those of states B and B' combined.

4 The Haldane-Shastry Model

4.1 Basic Properties

The Haldane-Shastry model was introduced independently by Haldane [12] and Shastry [13] in 1988. Haldane formulated the model as a Heisenberg XXZ model with inverse-square interaction, whereas Shastry analyzed the isotropic XXX model. In this work we concentrate on the XXX model. The Hamiltonian for a system of N sites can be written as

$$\mathcal{H}_{\mathrm{HS}} = \sum_{i=1}^{N-1} \sum_{j=i+1}^{N} J_{ij} \mathbf{S}_i \cdot \mathbf{S}_j, \qquad J_{ij} = J \left[\frac{N}{\pi} \sin \frac{\pi(i-j)}{N} \right]^{-2}. \tag{4.1}$$

The sites are assumed to form a ring the interaction falling off with the inverse square of the cord distance. This choice of the distance function imposes periodic boundary conditions on the system although the sum does explicitly not contain the boundary term with $\mathbf{S}_N \mathbf{S}_1$. The energy level spectrum is generated from the top down by so-called pseudomomenta $\{p_i\}$ that represent Yangian multiplet states and satisfy the following set of asymptotic Bethe ansatz equations:

$$N p_i = 2\pi I_i + \pi \sum_{j \neq i}^{M} \mathrm{sgn}(p_i - p_j), \qquad i = 1, \ldots, M, \tag{4.2}$$

where $0 \leq M \leq [N/2]$. Again $[\ldots]$ denotes the integer part of its argument. The Bethe quantum numbers I_i are integers for odd M and half-integers for even M on the interval

$$\frac{1}{2}(M+1) \leq I_i \leq N - \frac{1}{2}(M+1) \tag{4.3}$$

and the solutions of (4.2) are of the form

$$p_i = \frac{2\pi}{N} \bar{m}_i, \qquad \bar{m}_i \in \{1, 2, \ldots, N-1\}, \qquad \bar{m}_{i+1} - \bar{m}_i \geq 2. \tag{4.4}$$

The wave numbers and energies in terms of the pseudomomenta are

$$k = \frac{2\pi}{N} \sum_{i=1}^{M} \bar{m}_i \bmod (2\pi), \qquad E - E_{\mathrm{sv}} = 2 \left(\frac{\pi v_s}{N^2} \right) \sum_{i=1}^{M} \bar{m}_i (\bar{m}_i - N), \tag{4.5}$$

where $v_s = \pi J/2$ and E_{sv} is the spinon vacuum. The lowest energy level contains the maximum number of pseudomomenta. This level is unique if N is even and fourfold degenerate if N is odd. The pseudomomenta play a role similar to the fermions in the XX model.

4.2 Spinons: Energy and Motif

4.2.1 Energy

This section is directly based on the work by Haldane [42] and Talstra [43]. The energy spectrum of the Haldane-Shastry model can be written in terms of spinons. The ground state is the spinonic vacuum with energy

$$E_{\mathrm{sv}} = -\frac{\pi^2 J}{12} \left(N + \frac{2}{N} \right). \tag{4.6}$$

We denote the number of spinons present in any state by N_s and write N_+ and N_- for the numbers of up- and down-spinons. The number of spinons is then uniquely determined by the number of pseudomomenta and the magnetization and it holds

$$N_+ + N_- = N_s = N - 2M, \qquad N_+ - N_- = 2M_z. \tag{4.7}$$

The allowed values for the spinon orbital momenta are

$$\kappa_i = \frac{\pi}{N} m_i, \qquad m_i = -M, -M+2, \ldots, +M \tag{4.8}$$

which lead to a number of $2M+1 = 1 + (N - N_s)/2$ possible spinon orbitals. We specify a generic eigenstate by two different sets of quantum numbers for the momenta and spins,

$$\left\{ \begin{array}{c} -\frac{1}{2}(N-N_s) \le m_1 \le m_2 \le \cdots \le m_{N_s} \le \frac{1}{2}(N-N_s) \\ \sigma_1, \sigma_2, \ldots, \sigma_{N_s}, \qquad \sigma_i = \pm \end{array} \right\}. \tag{4.9}$$

The wave number and energy are independent of the individual spins, i.e., given by the momentum quantum numbers alone,

$$k = M\pi + \frac{\pi}{N} \sum_{i=1}^{N_s} m_i \mod 2\pi, \tag{4.10}$$

$$E = E_{\rm sv} + E_M + \sum_{i=1}^{N_s} \epsilon(m_i) + \frac{1}{N} \sum_{i<j} V(m_i - m_j) \tag{4.11}$$

with the vacuum energy (4.6) and

$$E_M = \frac{\pi v_s}{N^2} \left\{ \frac{1}{6} N(N^2+2) - \frac{1}{6} M \left[3N(N-1) - 4M^2 + 6M + 4 \right] \right\}, \tag{4.12}$$

$$\epsilon(m_i) = \frac{\pi v_s}{N^2} \left(M^2 - m_i^2 \right), \tag{4.13}$$

$$\frac{1}{N} V(m_i - m_j) = \frac{\pi v_s}{N^2} \left(M - |m_i - m_j| \right). \tag{4.14}$$

We observe an energy offset (4.12), a single-orbital contribution (4.13) and a pair interaction among the orbitals (4.14).

4.2.2 Motif

The structure of the spectrum is that of a Yangian symmetry algebra. For our purposes it suffices to know that the Yangian multiplet structure can be represented by a motif which simultaneously describes the pseudomomenta and the spin content of all states. We illustrate this connection in Tab. 1 for $N = 5$.

The motif of any eigenstate consists of binary strings of length N. The elements of each permissible string are a '10' (pseudomomentum) and a '0' (spinon). All consecutive '0's that do not belong to a '10' represent spinons in the same momentum state. Consecutive '10's represent pseudomomenta with $\Delta\bar{m}_i = 2$. Every '0' between two '10's increases $\Delta\bar{m}_i$ by one unit. Pseudomomenta with increasing $\bar{m}_i$ are encoded by successive '10's read from left to right. Spinons in orbitals with increasing m_i are encoded by successive '0's (separated by at least one '10') read from right to left. The spin content of any given Yangian multiplet can be read off the binary motif by recognizing the multiplets of the quantum number S_T representing the total spin in each spinon orbital. The degeneracy counts the different ways to distribute spins over the occupied orbitals.

In the XX case the motif pertains to individual eigenstates (Fig. 4) and encodes a specific spinon spin configuration.

motif	$\bar{m}_i$	m_i	k	E	spin	deg.	k_i
0 10 10	2, 4	2	1	$\frac{5}{2}$	$\frac{1}{2}$	2	2
10 0 10	1, 4	0	0	$\frac{13}{2}$	$\frac{1}{2}$	2	0
10 10 0	1, 3	-2	4	$\frac{5}{2}$	$\frac{1}{2}$	2	-2
00 10 0	3	$-1, 1, 1$	3	$\frac{21}{2}$	$\frac{1}{2} \otimes 1 = \frac{3}{2} \oplus \frac{1}{2}$	6	$-3, 1, 3$
0 10 00	2	$-1, -1, 1$	2	$\frac{21}{2}$	$\frac{1}{2} \otimes 1 = \frac{3}{2} \oplus \frac{1}{2}$	6	$-3, -1, 3$
000 10	4	$1, 1, 1$	4	$\frac{29}{2}$	$\frac{3}{2}$	4	$-1, 1, 3$
10 000	1	$-1, -1, -1$	1	$\frac{29}{2}$	$\frac{3}{2}$	4	$-3, -1, 1$
00000	–	$0, 0, 0, 0, 0$	0	$\frac{45}{2}$	$\frac{5}{2}$	6	$-4, -2, 0, 2, 4$

Table 1: List of motifs, pseudomomentum quantum numbers $\bar{m}_i$, spinon orbital momentum quantum numbers m_i, wave number k (in units of $2\pi/N$), energy $E - E_{\rm sv}$ (in units of $\pi v_s/N^2$), spin content, degeneracies, and spinon momenta k_i (in units of π/N) of all Yangian multiplets for $N = 5$.

4.3 Interacting Spinon Orbitals

In the previous section we have seen that the spinon quantum numbers are not neccessarily different. As in the XX model this observation is interpreted as an orbital structure and the spinon momenta $\kappa_i = \pi m_i/N$ are understood as orbital momenta. Each orbital can contain arbitrarily many spinons. This is clearly seen from Eq. (4.9). A state with M pseudomomenta contains $N - 2M$ spinons distributed over $M + 1$ orbitals. We will derive explicite expressions for the energy of states with a single orbital and also for the generic case of t orbitals.

4.3.1 Energy of a Single Orbital

A generic state with only one spinon orbital consists of a cluster of spinons between two blocks of pseudomomenta along the borders of the Brillouin zone. We sketch one such state in Fig. 13 for $N = 20$.

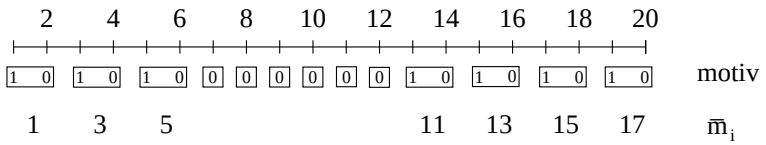

Figure 13: A generic state of the Haldane-Shastry model with a single orbit of spinons for $N = 20$ is shown. The first line gives the corresponding motif, showing the orbital of $N_s = 6$ spinons (squares around isolated zeros) imbedded between two blocks of pseudomomenta (oblongs containing '10'). The second line explicitely gives the pseudomomenta $\bar{m}_i$.

Generically the pseudomomenta take the values

$$\{\bar{m}_i\} = \left\{\bar{m}_1^-, \bar{m}_1^- + 2, \bar{m}_1^- + 4 \ldots \bar{m}_1^+, \bar{m}_2^-, \bar{m}_2^- + 2, \bar{m}_2^- + 4, \ldots \bar{m}_2^+\right\} \tag{4.15}$$

with the outer boundaries $\bar{m}_1^- = 1$ and $\bar{m}_2^+ = N - 3$. The inner boundaries $\bar{m}_1^+$ and $\bar{m}_2^-$ depend on the orbital momentum m of the spinon orbital,

$$\bar{m}_1^+ = \frac{1}{2}(N - N_s - 2m - 2), \qquad \bar{m}_2^- = \frac{1}{2}(N + N_s - 2m - 2). \tag{4.16}$$

We use (4.5) to calculate the energy of such a state. The sum over a cluster of pseudomomenta can be evaluated explicitely, giving

$$\begin{aligned} & \sum_{\{\bar{m}_i^-,\ldots,\bar{m}_i^+\}} \bar{m}_i^-(N - \bar{m}_i^-) \\ = \;& \alpha_i(\bar{m}_i^- - 2)(\bar{m}_i^- - 2 - N) + \alpha_i(\alpha_i + 1)(2\bar{m}_i^- - 4 - N) + \frac{2}{3}\alpha_i(\alpha_i + 1)(2\alpha_i + 1) \\ = \;& \alpha_i \bar{m}_i^-(\bar{m}_i^- - N) + \alpha_i^2(2\bar{m}_i^- - N) + \frac{4}{3}\alpha_i^3 + \mathcal{O}\left(N^2\right) \end{aligned} \tag{4.17}$$

where

$$\alpha_i = 1 + \frac{1}{2}(\bar{m}_i^+ - \bar{m}_i^-) \tag{4.18}$$

is the number of pseudomomenta in the i^{th} cluster. Inserting the pseudomomenta (4.16) yields

$$\sum_{\{\bar{m}_i^-,\ldots,\bar{m}_i^+\}} \bar{m}_i^-(N - \bar{m}_i^-) = \frac{1}{24}\left(3N^2N_s - 12N_sm^2 - 2N^3 - N_s^3\right) + \mathcal{O}\left(N^2\right) \tag{4.19}$$

and thus the energy

$$E = \frac{\pi v_s}{12N^2}\left(3N^2N_s - 12N_sm^2 - N_s^3\right) + \mathcal{O}\left(N^2\right). \tag{4.20}$$

We use the reduced quantities

$$\epsilon = \frac{E}{\pi v_s N}, \qquad n_s = \frac{N_s}{N}, \qquad \kappa = \frac{m}{N} \tag{4.21}$$

and write (4.20) as

$$\epsilon = \frac{n_s}{12}\left(3 - 12\kappa^2 - n_s^2\right) \tag{4.22}$$

which has been reported recently [39].

4.3.2 Energy of Multiple Orbitals

We extend the calculation of the previous section (4.3.1) to the case of multiple orbitals. The motif of such a state will contain t clusters of spinons separated by $t-1$ blocks of pseudomomenta. Each state may have one block of pseudomomenta at each border of the Brillouin zone. For definiteness we will assume that these blocks are present. We denote the minimum and maximum value of the i^{th} block of pseudomomenta by $\bar{m}_i^-$ and $\bar{m}_i^+$. Then the spinon content of the i^{th} orbital is given by

$$s_i = \bar{m}_{t+2-i}^- - \bar{m}_{t+1-i}^+ - 2, \qquad i = 1, \ldots, t. \tag{4.23}$$

The orbital momenta can be expressed via the $\bar{m}_i^\pm$ as well,

$$m_i = 2i - M + \sum_{l=1}^{i}\left(\bar{m}_{t+2-l}^+ - \bar{m}_{t+2-l}^-\right), \qquad i = 1, \ldots, t. \tag{4.24}$$

These equations for m_i and s_i can be inverted to express the pseudomomenta $\bar{m}_i^{\pm}$ via the orbital variables for momentum and filling,

$$\begin{aligned}
\bar{m}_1^- &= 1 && (4.25)\\
\bar{m}_j^- &= 1+N-M-m_{t+2-j}-\sum_{l=1}^{t+1-j} s_l, \qquad j=2,3,\ldots,t+1 && (4.26)\\
\bar{m}_j^+ &= -1-N-M-m_{t+1-j}-\sum_{l=1}^{t+1-j} s_l, \qquad j=1,2,\ldots,t && (4.27)\\
\bar{m}_{t+1}^+ &= N-1 && (4.28)
\end{aligned}$$

We simplify the exact expression (4.17) to

$$\sum_{\{\bar{m}_i^-,\ldots,\bar{m}_i^+\}} \bar{m}_i^-(N-\bar{m}_i^-) = \sum_{i=1}^{t+1} \frac{\alpha_i}{3}\Big[3(\bar{m}_i-2)(\bar{m}_i-N+2\alpha_i)+(\alpha_i+1)(4\alpha_i-3N+2)\Big] \qquad (4.29)$$

with

$$\alpha_i = 1+\frac{1}{2}(\bar{m}_i^+-\bar{m}_i^-) = \frac{1}{2}(m_{t+2-i}-m_{t+1-i}), \qquad i=2,\ldots,t \qquad (4.30)$$

and $\alpha_1=(N-N_s-2m_t)/4$ and $\alpha_{t+1}=N-\bar{m}_{t+1}^-+1$. The terms in the sum (4.29) can be evaluated exactly, but the first and last term must be treated separately since the according α's are different. The generic terms are found to be

$$\begin{aligned}
\Sigma_i &= \frac{m_i-m_{i-1}}{24}\Big[-3(N-m_i-\nu_{i-1}-2)(N+2m_{i-1}+\nu_{i-1}-2)\\
&\qquad +2(m_i-m_{i-1}+2)(2m_i-2m_{i-1}-3N+2)\Big] && (4.31)
\end{aligned}$$

for $1<i<t+1$. The first term is

$$\Sigma_1 = \frac{N-N_s-2m_t}{48}\Big[6(N+N_s+2m_t-2)-(N-N_s-2m_t+4)(2N+N_s+2m_t-2)\Big] \qquad (4.32)$$

and the last term is obtained from the first term by exchanging m_t with $-m_1$. With these Σ_i we have the exact energy (4.5) of any eigenstate expressed via the orbital variables m_i and ν_i. The formula reduces significantly in the thermodynamic limit and the limit process is easily performed. We give the reduced energy in the form it has been published in [39],

$$\begin{aligned}
\epsilon = \sum_{i=1}^{t-1}\frac{8}{3}\left[(a_{i,i+1}-\bar{\kappa}_i)^3-(a_{i,i+1}-\bar{\kappa}_{i+1})^3\right]+2\left[(a_{i,i+1}-\bar{\kappa}_{i+1})^2-(a_{i,i+1}-\bar{\kappa}_i)^2\right]\\
+\frac{8}{3}\left[(a_{t,t+1}-\bar{\kappa}_t)^3-(a_{0,1}-\bar{\kappa}_1)^3\right]+2\left[(a_{0,1}-\bar{\kappa}_1)^2-(a_{t,t+1}-\bar{\kappa}_t)^2\right], \qquad (4.33)
\end{aligned}$$

where $\bar{\nu}_j = s_j/N$ is the scaled filling and the functions

$$a_{i,k} = \frac{1}{4} - \frac{1}{4}\sum_{j=1}^{i}\nu_j + \frac{1}{4}\sum_{j=k}^{t}\nu_j, \quad i = 0,1,2,\ldots,t, \tag{4.34}$$

act as "local couplings". Again the ordered structure of the orbitals breaks the perfect symmetry. It is not possible to separate (4.33) into pair interactions because the couplings $a_{i,k}$ depend on all orbitals. Changing the spinon content of a single orbital will in general affect all couplings.

4.4 Thermodynamics

We start with the exact energy expression (4.11) which explicitly reads

$$E - E_{\mathrm{sv}} = \frac{\pi v_s}{12N^2}\big(3N^2N_s - N_s^3 + 4N_s\big) - \frac{\pi v_s}{N^2}\sum_{i=1}^{N_s} m_i(m_i - N_s - 1 + 2i), \tag{4.35}$$

shift the momenta m_i by $(N_s+1)/2+i$ and scale them by $2/N$ thereafter. This transformation maps our momenta m_i onto the discrete version of Haldane's rapidity x in [42]. Then the sum reduces to a sum over third binomials and cancels the N_s^3 in the first summand. Ignoring all finite-size corrections we immediately obtain the energy expression

$$E - E_{\mathrm{sv}} \;=\; \frac{N_s\pi v_s}{4} - \frac{\pi v_s}{4}\sum_{i=1}^{N_s} x_i^2 + \mathcal{O}\left(1\right) \;=\; \frac{N\pi v_s}{4}\sum_{i=1}^{N_s}\left(1 - x_i^2\right) + \mathcal{O}\left(1\right) \tag{4.36}$$

with

$$x_i = \frac{2}{N}\Big(\frac{N_s+1}{2} - i\Big), \qquad -1 \le x_1 < x_2 < \cdots < x_{N_s} \le +1. \tag{4.37}$$

It is built up of the spinon dispersion function

$$\epsilon(x) = \frac{\pi v_s}{4}\big(1 - x^2\big) \tag{4.38}$$

in agreement with [42]. In the thermodynamic limit one is no longer interested in single particles but works with particle densities instead. We therefore define the spinon density $n(x) = n_+(x) + n_-(x)$ which decomposes into separate functions for spin-up and spin-down spinons each. In the transition from the discrete x_i to the continuous variable x all sums become integrals,

$$\frac{1}{N}\sum_{i=1}^{N_s} \longrightarrow \int_{-1}^{+1}\mathrm{d}x. \tag{4.39}$$

The inner energy per site can then be written as the integral over the two dispersions,

$$u = \sum_{\sigma\in\{+,-\}}\int_{-1}^{+1}\mathrm{d}x\; n_\sigma(x)\epsilon(x). \tag{4.40}$$

The entropy s per site can be found by the usual procedure of counting states. A fermionic construction is possible since all x_i are distinct. The only complication arises from the fact that spin-up spinons and spin-down-spinons must be distinguished. We arive, however, at

$$s = -\frac{k_B}{2}\int_{-1}^{+1}\mathrm{d}x\,\Big[2n(x)\ln\big(2n(x)\big) + \big(1-2n(x)\big)\ln\big(1-2n(x)\big)\Big]. \tag{4.41}$$

With these ingredients and the inverse temperature $\beta = 1/(k_B T)$ the Helmholtz free energy per site reads

$$a = u - Ts = \int_{-1}^{+1} \mathrm{d}x \, \Big(n(x)\epsilon(x) + \frac{1}{2\beta} \Big[2n(x) \ln\big(2n(x)\big) + \big(1-2n(x)\big) \ln\big(1-2n(x)\big) \Big] \Big). \tag{4.42}$$

The variation for n_+ and n_- is given by

$$\frac{\delta a}{\delta n_+} = \frac{\delta a}{\delta n_-} = \int_{-1}^{+1} \mathrm{d}x \, \Big(\epsilon(x) + \frac{1}{\beta} \Big[\ln\big(2n(x)\big) - \ln\big(1-2n(x)\big) \Big] \Big) \tag{4.43}$$

and vanishes only for

$$\epsilon(x) + \frac{1}{\beta} \ln \frac{2n(x)}{1-2n(x)} = 0 \quad \Longleftrightarrow \quad n(x) = \frac{1}{2\big(\mathrm{e}^{\beta\epsilon(x)}+1\big)}. \tag{4.44}$$

It is clear by (4.43) that both polarized spinon densities are the same, $n_\sigma(x) = n(x)/2$, $\sigma = \pm$. From the combination of (4.42) and (4.44) we have

$$a(\beta) = -\frac{1}{2\beta} \int_{-1}^{+1} \mathrm{d}x \, \ln\big(1+\mathrm{e}^{-\beta\epsilon(x)}\big) \tag{4.45}$$

and all thermodynamic properties of the Haldane-Shastry model follow as long as no magnetic field is applied.
Haldane has given explicit results for the thermodynamics of this model before. Our result (4.44) is in accordance with his statements in [42]. We give some details of his calculation in App. D.

5 Summary, Conclusion, and Outlook

In Sec. 2 we have given a short introduction to the solution of the anisotropic spin-1/2 XXZ Heisenberg model with uniform nearest-neighbor exchange, anisotropy parameter Δ and periodic boundary conditions. The coordinate Bethe ansatz and the algebraic Bethe ansatz as solutions of the model are sketched. This provides the framwork for the definition of the dynamic spin-structure factors $S_{\mu\nu}(q,\omega)$ as auto-correlation functions.

The main part of the work is given in Sec. 3 where we specialize to the critical point $\Delta = 0$, known as the XX model. We take two aspects into focus, (i) the description of the excitation spectrum by quasiparticles and (ii) the large-size asymptotics of the said structure factors.

In two short subsections the well-known quasiparticles – magnons and fermions – are described following present literature. Then spinons are precisely defined and many interesting properties are shown including their particle and orbital interaction, relation to a knew Bethe ansatz scheme, semionic exclusion statistics and thermodynamics. Many results are knew and have been published recently [34, 39]. The derivation of Bethe ansatz equations in terms of spinons suggests that a completely spinonic solution of the XX model should be possible although the wave functions have not been calculated that way yet. The section on thermodynamics does not reveal knew information about the model since it has been analyzed more than forty years ago [35] but again a solely spinonic approach deepens our understanding of this rather knew species of quasiparticles.

The next section deals with the dynamic spin structure factor $S_{-+}(q,\omega)_0$ which increases the number of spinons by one. We propose an extension of a compact exact result from an earlier study [18] to the whole spectrum and use it to present extensive numerical data for the total spectral intensity of excitations with up to four spinons. We analyze both even and odd chains but restrict ourself to transitions from the ground state. The work could easily be extended to the spin structure factor $S_{+-}(q,\omega)_0$ which decreases the number of spinons by one. It should not be too difficult to extend the exact results to excitations with more spinons since many features of the general formulas can be guessed already. But as soon as more that two spinons are present, the spectral distribution in the (q,ω) plane becomes intricate; singularities at inner folds appear and it is no longer possible to express the results by the physical quantities of transferred energy ω and wave number q alone. The extension from [18] is a good guess which has been checked numerically to fulfill several sum rules. Nevertheless a rigorous proof is still missing since the approach taken in 2004 [18] failed. A new attempt in the framework of free fermions might be more promising.

The second part of the analysis is done numerically. We analyze the large-N limit of the said spin structure factor and find the contributions of the smallest classes of excitations all vanishing. Thus no numerical evidence for the survival of any single excitation class is found and further numerical analysis does not appear interesting.

Sec. 4 is devoted to the Haldane-Shastry model, a modification of the XXX model with inverse-square interaction. This model is also open to the analysis by spinons. We state the properties of spinons more clearly then Haldane has given them in [12]. Analogously to the previos section we demonstrate how a Bethe ansatz emerges from the spinonic energy formula. Again we do not proceed to the calculation of wave functions. But we do derive new formulas for the interaction of spinonic orbitals. The energy of arbitrarily many orbitals is precisely formulated. We see that it does not decompose into a sum of two-orbital interaction terms. In the last subsection (4.4) we analyze the thermodynamics of the Haldane-Shastry model in terms of spinons. Correct results are obtained for the model without an external magnetic field. For the case of a magnetic field results have been given by Haldane [42] but we could not reproduce them yet. If they are correct a solution of the variation problem must exist although it eluded us so far.

Last we present six appendices. App. A gives a detailed derivation of an interesting constant which appears in our formulas for the dynamic spin structure factors and is known from other studies [44]. App. B presents some details of a special function named $\phi(x)$ which largely dictates the functional

dependence of the transition-rates on the spinons. Then App. C works out an interesting binomial identity which was used to prove the completeness of the spinonic spectrum in Sec. 3.3.2. Some calculations of Sec. 3.3.5 are moved to Appendix E and we give some details of Haldans's results for the thermodynamics of the Haldane-Shastry model in App. D. Finally we give a short appendix on the theoretical background of neutron optics. There we sketch how the knowledge of dynamic spin structure factors helps to design experimental the set-up for the analysis of solid states. The structure factors are directly open to neutron scattering experiments and thus provide experimentally accessable key information on the inner structure of materials.

Acknowledgements

With great pleasure I would like to thank PD Dr. Michael Karbach who made this work possible. He kindled my interest in one-dimensional condensed matter physics and the theory of exactly solvable models. With constant interest and support he accompanied me through five interesting years of research. I greatfully appreciate the oportunity of visiting many interesting and stimulating conferences during my PhD time which he made possible.
I am also deeply indebted to Prof. Dr. Gerhard Müller from University of Rhode Island who hosted me as a guest for one year. From him I learned a lot about quasiparticles and their statistics and he also introduced me to the Haldane-Shastry model. With paternal care he guided me through a maior part of the present work.
Then I would like to thank Prof. Dr. Andreas Klümper and the Many-Particle-Group at Wuppertal for many fruitful discussions and the warm atmosphere at the institute. They have been both collegues and friends to me for several years.
Also do I wish tho thank Dr. Mitsuhiro Arikawa from the Graduate School of Pure and Applied Sciences at University of Tsukuba who valuably participated in the project [34] and first introduced the ϕ-function.
Financial support from the *Graduiertenkolleg Darstellungstheorie und ihre Anwendungen in der Physik* is greatfully appreciated. The joint work with the mathematicians broadend my horizon and stimulated my interest in the algebra behind the physical models.
Special thanks are due to PD. Dr. Andreas Fledderjohann for many interesting discussions and Dr. Stefan Glocke and Roland Olbricht for proofreading parts of the manuscript.

Declaration

Hereby do I declare that the PhD thesis with the title: *Quasiparticles, Dynamics and Thermodynamics in the XX chain* is my own original work. All used sources are listed and lest stated otherwise all work contained within the thesis is my own independent research. I agree with making the thesis publicly available.

Wuppertal, on the 4th of January

Klaus Wiele

A The Scaling Factor $M^-\big(\{k_i^0\},\{k_i^-\}\big)$ for Even N

The scaling factor is given by

$$M^-\big(\{k_i^0\},\{k_i^-\}\big) = \frac{\left(\prod_{i<j}^{r-1}\sin\frac{k_i^- - k_j^-}{2}\right)^2\left(\prod_{i<j}^{r}\sin\frac{k_i^0 - k_j^0}{2}\right)^2}{N^{2r-2}\left(\prod_{i=1}^{r}\prod_{j=1}^{r-1}\sin\frac{k_i^0 - k_j^-}{2}\right)^2} \tag{A.1}$$

where the momenta are

$$k_i^0 = \frac{\pi}{N}\bar m_i^0, \qquad i=1,\ldots,r \qquad \text{and} \qquad k_i^- = \frac{\pi}{N}\bar m_i^-, \qquad i=1,\ldots,r-1 \tag{A.2}$$

with

$$\{\bar m_i^0\} = \left\{\frac{N}{2}+1,\frac{N}{2}+3,\ldots,\frac{3N}{2}-1\right\} = \left\{\frac{N}{2}-1+2i,\ \ i=1,2,\ldots,\frac{N}{2}\right\}, \tag{A.3}$$

$$\{\bar m_i^-\} = \left\{\frac{N}{2}+2,\frac{N}{2}+4,\ldots,\frac{3N}{2}-2\right\} = \left\{\frac{N}{2}+2i,\ \ i=1,2,\ldots,\frac{N}{2}-1\right\}. \tag{A.4}$$

according to Fig. 6. For transition from the ground state we have $r = N/2$ which is compatible with the definition (2.58). With these explicit momenta the scaling factor can be simplified to

$$\begin{aligned} & M^-\left(\{k_i^-\},\{k_i^0\}\right) \\ = \ & N^{2-2r}\frac{\left(\prod_{k=1}^{r-2}\left[\sin\left(\frac{k\pi}{N}\right)\right]^{2(r-k-1)}\right)\left(\prod_{k=1}^{r-1}\left[\sin\left(\frac{k\pi}{N}\right)\right]^{2(r-k)}\right)}{\left(\prod_{k=1}^{r-1}\left[\sin\frac{\pi}{N}\left(k-r+\frac12\right)\right]^{2k}\right)\left(\prod_{k=1}^{r-1}\left[\sin\frac{\pi}{N}\left(k-r-\frac12\right)\right]^{2k}\right)} \\ = \ & N^{2-N}\prod_{k=1}^{N/2}\frac{\left[\sin\left(\frac{k\pi}{N}\right)\right]^{2N-4k-2}}{\left[\sin\frac{\pi}{N}\left(k-\frac12\right)\right]^{2N-4k}}. \end{aligned} \tag{A.5}$$

Using the exact expressions

$$\prod_{k=1}^{N/2}\sin^2\left(\frac{k\pi}{N}\right) = N\cdot 2^{1-N} \qquad \text{and} \qquad \prod_{k=1}^{N/2}\sin^2\frac{\pi}{N}\Big(k-\frac12\Big) = 2^{1-N} \tag{A.6}$$

some products can be evaluated analytically, leaving only

$$M^-\left(\{k_i^-\},\{k_i^0\}\right) = \sqrt{N}\prod_{k=1}^{N/2}\frac{\sin^{4k-3}\eta(k-1/2)}{\sin^{4k-1}\eta k} = \sqrt{N}\,C_N(N/2) \tag{A.7}$$

with

$$C_N(n) = \prod_{k=1}^{n}\frac{\sin^{4k-3}\eta(k-1/2)}{\sin^{4k-1}\eta k} \qquad \text{and} \qquad \eta = \frac{\pi}{N}. \tag{A.8}$$

In the form of (A.7) the scaling factor has been published in [34]. The square root divergency has been isolated and the remaining product tends towards a constant in the limit $N \to \infty$.
In the following the asymptotic expansion shall be sketched. We add the missing factors so as to get the same number of factors in the nominator and denominator, and expand the nominator,

$$\begin{aligned} C_N(N/2) &= 2^{N-1}\sqrt{N} \prod_{k=1}^{N/2} \left[\frac{\sin\left(\frac{k\pi}{N} - \frac{\pi}{2N}\right)}{\sin\left(\frac{k\pi}{N}\right)} \right]^{4k} \\ &= 2^{N-1}\sqrt{N} \prod_{k=1}^{N/2} \left[\cos\left(\frac{\pi}{2N}\right) - \cot\left(\frac{k\pi}{N}\right) \sin\left(\frac{\pi}{2N}\right) \right]^{4k}. \end{aligned} \tag{A.9}$$

We apply the natural logarithm thereby turning the product into a sum and obtain

$$\begin{aligned} & \ln M^{-}\left(\{k_i^{-}\}, \{k_i^{0}\}\right) \\ = \; & \ln(N) + (N-1)\ln(2) + 4\sum_{k=1}^{N/2} k \ln\left[\cos\left(\frac{\pi}{2N}\right) - \cot\left(\frac{k\pi}{N}\right) \sin\left(\frac{\pi}{2N}\right) \right]. \end{aligned} \tag{A.10}$$

To further expand the remaining sum the different behavior at the lower and upper border must be taken into consideration. We want to replace the functions by their Taylor series expansion around zero (cotangent) and unity (logarithm) wherever possible.

- At the lower border ($k = 1$) the argument of the cotangent tends to zero and we can expand the cotangent. But the logarithm shall not be expanded there since its argument tends toward one half. Instead we will use a well-known series expansion from literature.
- At the upper border ($k = N/2$) the argument of the cotangent tends towards $\pi/2$ and we do not expand there. But as the cotangent itself vanishes the argument of the logarithm in turn tends towards unity and the logarithm shall be expanded. The remaining cotangent expressions shall be turned into integrals with the Euler-Maclaurin formula.

First we break the sum apart into upper and lower part. As separation between the two parts we choose

$$m = \left[\sqrt{N}\right] \tag{A.11}$$

where again $[\ldots]$ denotes the integer part of the argument. The lower part of the sum becomes

$$\begin{aligned} & \sum_{k=1}^{m} k \ln\left[\cos\left(\frac{\pi}{2N}\right) - \cot\left(\frac{k\pi}{N}\right) \sin\left(\frac{\pi}{2N}\right) \right] \\ = \; & \sum_{k=1}^{m} k \ln\left[\left(1 + \mathcal{O}\left(N^{-2}\right)\right) - \left(\frac{\pi}{2N} + \mathcal{O}\left(N^{-3}\right)\right)\left(\frac{N}{k\pi} - \frac{k\pi}{3N} + \mathcal{O}\left(k/N\right)^3\right) \right] \\ = \; & \sum_{k=1}^{m} k \ln\left[1 - \frac{1}{2k} + \frac{k\pi}{6N^2} + \mathcal{O}\left(N^{-2}\right) \right] \\ = \; & \sum_{k=1}^{m} \left[k \ln\frac{2k-1}{2k} + k \ln\left(1 + \frac{k^2\pi^2}{3(2k-1)N^2} + \mathcal{O}\left(N^{-2}\right)\right) \right] \\ = \; & \sum_{k=1}^{m} \left[k \ln\frac{2k-1}{2k} + \frac{k^3\pi^2}{3(2k-1)N^2} + \mathcal{O}\left(k \cdot N^{-2}\right) \right]. \end{aligned} \tag{A.12}$$

The logarithmic expression contains the divergency at the lower border. It is evaluated using the well-known expansion [45]

$$\sum_{k=1}^{m} k\ln k = \ln g + \frac{\ln m}{12}\left(6n^2+6n+1\right) - \frac{m^2}{4} - \frac{1}{4}\sum_{k=1}^{\infty}\frac{n^{-2k}B_{2k+2}}{k(k+1)(2k+1)} \tag{A.13}$$

where

$$g = \exp\left(\frac{1}{12} - \zeta'(-1)\right) = 1.282\,427\,129\,100\,\ldots \tag{A.14}$$

is Gleisher's constant [46] and B_k are the Bernoulli numbers [47]. Thus we arrive at

$$\begin{aligned}&\sum_{k=1}^{m} k\ln\left[\cos\left(\frac{\pi}{2N}\right) - \cot\left(\frac{k\pi}{N}\right)\sin\left(\frac{\pi}{2N}\right)\right]\\ =\;& -\frac{m}{2} - \frac{\ln m}{8} - \frac{3g}{2} + \frac{7\ln 2}{24} - \frac{1}{48m} + \frac{\pi^2 m^3}{18N^2} + \mathcal{O}\left(N^{-1}\right).\end{aligned} \tag{A.15}$$

The upper part of the sum becomes

$$\begin{aligned}&\sum_{k=m+1}^{N/2} k\ln\left[\cos\left(\frac{\pi}{2N}\right) - \cot\left(\frac{k\pi}{N}\right)\sin\left(\frac{\pi}{2N}\right)\right]\\ =\;& \sum_{k=m+1}^{N/2} k\ln\cos\left(\frac{\pi}{2N}\right) + \sum_{k=m+1}^{N/2} k\ln\left[1-\tan\left(\frac{\pi}{2N}\right)\cot\left(\frac{k\pi}{N}\right)\right]\end{aligned} \tag{A.16}$$

where

$$\sum_{k=m+1}^{N/2} k\ln\cos\left(\frac{\pi}{2N}\right) = -\frac{\pi^2}{64} + \mathcal{O}\left(N^{-1}\right) \tag{A.17}$$

and

$$\sum_{k=m+1}^{N/2} k\ln\left[1-\tan\left(\frac{\pi}{2N}\right)\cot\left(\frac{k\pi}{N}\right)\right] = -\sum_{k=m+1}^{N/2} k\left\{\sum_{l=1}^{\infty}\frac{1}{l}\left[\tan\left(\frac{\pi}{2N}\right)\cot\left(\frac{k\pi}{N}\right)\right]^l\right\}. \tag{A.18}$$

Using the Euler-Maclaurin expansion formula we obtain

$$\begin{aligned}\sum_{k=m+1}^{N/2} k\cot\left(\frac{k\pi}{N}\right) &= \frac{N^2\ln 2}{2\pi} - \frac{mN}{\pi} - \frac{N}{2\pi} + \frac{m^3\pi}{9N} + \mathcal{O}(1)\\ \sum_{k=m+1}^{N/2} k\cot^2\left(\frac{k\pi}{N}\right) &= \frac{N^2}{\pi^2}\ln\frac{N}{m\pi} + \frac{N^2}{\pi^2}\left(1-\frac{\pi^2}{8}\right) - \frac{N^2}{2m\pi^2} + \mathcal{O}(N)\\ \sum_{k=m+1}^{N/2} k\cot^3\left(\frac{k\pi}{N}\right) &= \frac{N^3}{m\pi^3} + \mathcal{O}\left(N^2\right)\end{aligned} \tag{A.19}$$

for the relevant terms and thus

$$\begin{aligned}
&\sum_{k=m+1}^{N/2} k \ln\left[\cos\left(\frac{\pi}{2N}\right) - \cot\left(\frac{k\pi}{N}\right)\sin\left(\frac{\pi}{2N}\right)\right] \\
= \; & -\frac{N\ln 2}{4} + \left(\frac{m}{2} - \frac{m^3\pi^2}{18N^2}\right) + \frac{1}{8}\ln\frac{m}{N} + \frac{1+\ln\pi}{8} + \frac{1}{48m} + \mathcal{O}\left(N^{-1}\right) \qquad \text{(A.20)}
\end{aligned}$$

which in combination with (A.15) leads to

$$\begin{aligned}
&\sum_{k=1}^{N/2} k \ln\left[\cos\left(\frac{\pi}{2N}\right) - \cot\left(\frac{k\pi}{N}\right)\sin\left(\frac{\pi}{2N}\right)\right] \\
= \; & -\frac{N\ln 2}{4} - \frac{\ln N}{8} + \left(\frac{1+\ln\pi}{8} - \frac{3g}{2} + \frac{7\ln 2}{24}\right) + \mathcal{O}\left(N^{-1}\right). \qquad \text{(A.21)}
\end{aligned}$$

The scaling factor reduces in the thermodynamic limit to the compact expression

$$\begin{aligned}
M^-\left(\{k_i^-\},\{k_i^0\}\right) &= \sqrt{N}\exp\left(\frac{\ln 2}{6} - 6g + \frac{1+\ln\pi}{2}\right) \\
&= \sqrt{N}\,\sqrt{\pi}\exp\left(\frac{\ln 2}{6} + \zeta'(-1)\right) \\
&= \sqrt{N} \times 0.737\,390\,711\,766\ldots \qquad \text{(A.22)}
\end{aligned}$$

where we have used (A.14) in the second step.

B The Function $\phi(n)$

The function $\phi(n)$ is defined by

$$\phi(n) = \left(\prod_{k=1}^{n} \frac{\sin\left(\frac{k\pi}{N} - \frac{\pi}{2N}\right)}{\sin\left(\frac{k\pi}{N}\right)} \right)^2 \quad \text{for } n = 1, 2, \ldots, N/2 \qquad \text{and} \qquad \phi(0) = 1. \tag{B.1}$$

We regard $N \in \mathbb{N}$ as a fixed external parameter. Then $\phi(n)$ decreases strictly monotonically from unity to $1/N$. Besides the sharp maximum at $n = 0$ the function is flat and featureless.

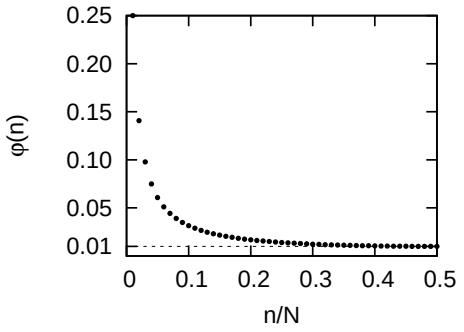

Figure 14: The function $\phi(n)$ for $N = 100$ and $n = 1, 2, \ldots, 50$. The dashed line marks the minmimum value $\phi(N/2) = 1/N$. The point $\phi(0)$ is not displayed.

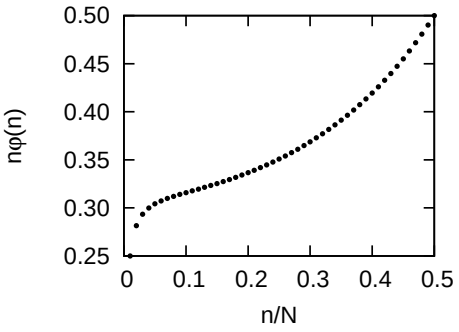

Figure 15: The scaled function $n\phi(n)$ for N=100. The kink at the left becomes ever sharper with increasing N.

In this section we sketch the asymptotic expansion for large N when the argument lies within the range $\sqrt{N} \le n \le N/2 - \sqrt{N}$. Again we use the threshold $m = [\sqrt{N}\,]$ and write

$$\begin{aligned} \ln \phi(n) &= 2 \sum_{k=1}^{n} \ln \left[\cos\left(\frac{\pi}{2N}\right) - \sin\left(\frac{\pi}{2N}\right) \cot\left(\frac{k\pi}{N}\right) \right] \\ &= 2n \ln \cos\left(\frac{\pi}{2N}\right) + 2 \sum_{k=1}^{n} \ln \left[1 - \tan\left(\frac{\pi}{2N}\right) \cot\left(\frac{k\pi}{N}\right) \right]. \end{aligned} \tag{B.2}$$

The first term reduces to

$$2n \ln \cos\left(\frac{\pi}{2N}\right) = \frac{n\pi^2}{4N^2} + \mathcal{O}\left(n \cdot N^{-4}\right) \tag{B.3}$$

and the sum is again split into two with

$$\begin{aligned} \sum_{k=1}^{m} \ln \left[1 - \tan\left(\frac{\pi}{2N}\right) \cot\left(\frac{k\pi}{N}\right) \right] &= \sum_{k=1}^{m} \ln \left[1 - \left(\frac{\pi}{2N} + \mathcal{O}\left(N^{-3}\right) \right) \left(\frac{N}{k\pi} + \mathcal{O}\left(k \cdot N^{-1}\right) \right) \right] \\ &= \sum_{k=1}^{m} \ln \frac{2k-1}{2k} + \mathcal{O}\left(N^{-1}\right) \\ &= -\frac{1}{2} \ln(m\pi) - \frac{1}{8m} + \mathcal{O}\left(N^{-1}\right) \end{aligned} \tag{B.4}$$

and

$$\begin{aligned}
&\sum_{k=m+1}^{n} \ln\Big[1-\tan\Big(\frac{\pi}{2N}\Big)\cot\Big(\frac{k\pi}{N}\Big)\Big] \\
= \;& -\sum_{k=m+1}^{n}\sum_{l=1}^{\infty}\frac{1}{l}\Big[\tan\Big(\frac{\pi}{2N}\Big)\cot\Big(\frac{k\pi}{N}\Big)\Big]^{l} \\
= \;& \frac{1}{2}\ln\frac{N}{m\pi}+\frac{1}{2}\ln\sin\frac{n\pi}{N}-\frac{\pi}{4N}\cot\frac{n\pi}{N}+\mathcal{O}\left(N^{-1}\right). \qquad \text{(B.5)}
\end{aligned}$$

The result is

$$\phi(n)=\frac{1}{N\sin\frac{n\pi}{N}}\;\exp\Big(\frac{\pi}{4N}\cot\frac{n\pi}{N}\Big)\times\big[1+\mathcal{O}\left(1/N\right)\big],\qquad \sqrt{N}\le n\le N/2-\sqrt{N} \qquad \text{(B.6)}$$

where the order of the argument of the exponential function varies between $1/m$ and m/N^2 according to the value of n.

C A Useful Binomial Identity

In Sec. 3.3.2 the sum

$$S = \sum_{N_+=0}^{N_s} \binom{A+N_+-1}{N_+}\binom{A+N_--1}{N_-}, \qquad A = 1+\frac{N-N_s}{2}, \qquad N_+ + N_- = N_s \tag{C.1}$$

has to be calculated. We set $N = 2M$ and $N_s = 2L$ to obtain

$$S = \sum_{N_+=0}^{N_s} \binom{N_+ + M - L}{N_+}\binom{M+L-N_+}{N_-}. \tag{C.2}$$

Now we shift the index of summation, $k = N_+ - L$, and use the identity [47]

$$\binom{n}{k} = (-)^k \binom{k-n-1}{k} \tag{C.3}$$

to remove the summation index from the "nominators:"

$$S = \sum_{k=-L}^{+L} \binom{M+k}{L+k}\binom{M-k}{L-k} = \sum_{k=-L}^{+L} \binom{L-M-1}{L+k}\binom{L-M-1}{L-k}. \tag{C.4}$$

Shifting back the sum ($k \to k+L$) yields

$$S = \sum_{k=0}^{2L} \binom{L-M-1}{k}\binom{L-M-1}{2L-k} \tag{C.5}$$

which is a special case of [40]

$$\sum_{k=0}^{p} \binom{n}{k}\binom{m}{p-k} = \binom{n+m}{p} \tag{C.6}$$

with $n = m = L-M-1$ and $p = 2L$. Thus we obtain

$$S = \sum_{k=0}^{2L} \binom{L-M-1}{k}\binom{L-M-1}{2L-k} = \binom{2L-2M-2}{2L} = \binom{2M+1}{2L} = \binom{N+1}{N_s} \tag{C.7}$$

where we use (C.3) in the last step.

D Thermodynamics of the Haldane-Shastry Model

We have given the Helmholtz free energy of the Haldane-Shastry model in the main text (4.42). It determines the thermodynamics of the model without a magnetic field. In this appendix we compare our result to that one previously given by Haldane in [42].
He gives the thermodynamics in the presence of a magnetic field h but the formulas are distorted by some misprints. Especially his spinon density (Eq. (3.10) in [42]) is definitely wrong in the limit $h \to 0$. We therefore start with his definition of the quantity $\mu(x)$ which has the meaning of a chemical potential,

$$\frac{\sinh\big(\beta h \mu(x)/2\big)}{\sinh\big(\beta h/2\big)} = \mathrm{e}^{-\beta\epsilon(x)}, \qquad \beta = \frac{1}{k_B T}. \tag{D.1}$$

The dispersion

$$\epsilon(x) = \frac{\pi v_s}{4}\big(1-x^2\big), \qquad -1 \le x \le +1 \tag{D.2}$$

is the same as in (4.38). In the limit $h \to 0$ the chemical potential reduces to

$$\mu(x) = \mathrm{e}^{-\beta\epsilon(x)} \tag{D.3}$$

where the argument x is always the continuous version of our discrete rapidity x_i from (4.37). Haldane's Gibbs free energy

$$f(\beta,h) = -\frac{1}{2\beta}\int_{-1}^{+1}\mathrm{d}x\,\ln\left(\frac{\sinh\big(\beta h(1+\mu(x))/2\big)}{\sinh\big(\beta h/2\big)}\right) \tag{D.4}$$

coincides with our result (4.45) for the Helmholtz free energy in the limit $h \to 0$. It also yields an expression for the entropy per site in the presence of a magnetic field. From (D.4) we derive

$$s = \frac{k_B}{2}\int_{-1}^{+1}\mathrm{d}x\,\left\{\ln\frac{\sinh H[1+\mu(x)]}{\sinh H} - H\tanh H\mu(x) + \frac{\tanh H\mu(x)}{\tanh H[1+\mu(x)]}\ln\frac{\sinh H}{\sinh H\mu(x)}\right\} \tag{D.5}$$

with the reduced magnetic field $H = \beta h/2$ using $s = -\frac{\partial f}{\partial T}$.

E Thermodynamics with Spinons

In Sec. 3.3.5 the Gibbs free energy per site of the XX model is found to be s

$$g(T,h) = \sum_{\sigma} \int_{-\sigma\pi m_z}^{\pi+\sigma\pi m_z} \frac{\mathrm{d}k}{2\pi} \Big\{ \rho_\sigma(k) \sin k + k_B T \Big[\rho_\sigma(k) \ln \rho_\sigma(k) + \big(1-\rho_\sigma(k)\big) \ln \big(1-\rho_\sigma(k)\big) \Big] - \frac{h}{2} \sigma \rho_\sigma(k) \Big\} - \frac{1}{\pi} \cos(\pi m_z). \quad \text{(E.1)}$$

The summand with $\sigma = +$ may remain unaltered,

$$g_+(T,h) = \int_{-\pi m_z}^{\pi+\pi m_z} \frac{\mathrm{d}k}{2\pi} \Big\{ \rho_+(k) \sin k + k_B T \Big[\rho_+(k) \ln \rho_+(k) + \big(1-\rho_+(k)\big) \ln \big(1-\rho_+(k)\big) \Big] - \frac{h}{2} \rho_+(k) \Big\} - \frac{1}{\pi} \cos(\pi m_z). \quad \text{(E.2)}$$

In the other summand the range of integration is shifted by the substitution $k = k' - \pi$ and $\rho_-(k'-\pi) = 1 - \rho_+(k')$ is used to obtain

$$g_-(T,h) = \int_{\pi+\pi m_z}^{2\pi-\pi m_z} \frac{\mathrm{d}k}{2\pi} \Big\{ -\big(1-\rho_+(k')\big) \sin k' + k_B T \Big[\rho_+(k') \ln \rho_+(k') + \Big(1-\rho_+(k')\Big) \ln \Big(1-\rho_+(k')\Big) \Big] + \frac{h}{2} \big(1-\rho_+(k')\big) \Big\}. \quad \text{(E.3)}$$

Now we add both integrals. All terms containing the density function ρ_+ are the same and thus yield a single integral over the range $[-\pi m_z, 2\pi - \pi m_z]$. Since the density function and the sine are both periodic with period 2π we integrate over exactly one period and may therefore shift the range of integration arbitrarily. The integral over $-\sin k'$ can be solved and cancels the cosine of the magnetization outside the integral. The integral over $h/2$ yields $h/4 - hm_z/2$. We thus arrive at

$$g(T,h) = \int_{-\pi}^{+\pi} \frac{\mathrm{d}k}{2\pi} \Big\{ \rho_+(k) \sin k + k_B T \Big[\rho_+(k) \ln \rho_+(k) + \big(1-\rho_+(k)\big) \ln \big(1-\rho_+(k)\big) \Big] - \frac{h}{2} \rho_+(k) \Big\} + \frac{h}{4} - \frac{hm_z}{2}. \quad \text{(E.4)}$$

The relation (3.53) between the density functions has been used to express the Gibbs free energy by ρ_+ alone. In the same way we can write $g(T,h)$ as a function of ρ_-:

$$g(T,h) = \int_{-\pi}^{+\pi} \frac{\mathrm{d}k}{2\pi} \Big\{ \rho_-(k) \sin k + k_B T \Big[\rho_-(k) \ln \rho_-(k) + \big(1-\rho_-(k)\big) \ln \big(1-\rho_-(k)\big) \Big] + \frac{h}{2} \rho_-(k) \Big\} - \frac{h}{4} - \frac{hm_z}{2}. \quad \text{(E.5)}$$

Now we combine both expressions for g, writing $g = (g[\rho_+] + g[\rho_-])/2$, and obtain

$$\begin{aligned} g(T,h) &= \frac{1}{2}\sum_\sigma \int_{-\pi}^{+\pi} \frac{\mathrm{d}k}{2\pi} \Big\{ \rho_\sigma(k) \sin k + k_B T \Big[\rho_\sigma(k) \ln \rho_\sigma(k) + \big(1-\rho_\sigma(k)\big) \ln \big(1-\rho_\sigma(k)\big) \Big] \\ &\quad + \frac{h}{2} \rho_\sigma(k) \Big\} - \frac{h m_z}{2}. \end{aligned} \tag{E.6}$$

So far we have succeeded in removing the magnetization from the limits of integration in (E.1) but it has still survived outside the integral. But we can replace the magnetization by the integral (3.47). Then we perform the same steps as with the integrals in the Gibbs free energy, and obtain after obvious calculations

$$m_z[\rho_-] = +\frac{1}{2} - \int_{-\pi}^{+\pi} \frac{\mathrm{d}k}{2\pi} \rho_-(k), \qquad m_z[\rho_+] = -\frac{1}{2} + \int_{-\pi}^{+\pi} \frac{\mathrm{d}k}{2\pi} \rho_+(k), \tag{E.7}$$

$$m_z = \frac{m_z[\rho_-] + m_z[\rho_+]}{2} = \frac{1}{2} \sum_\sigma \int_{-\pi}^{+\pi} \frac{\mathrm{d}k}{2\pi} \sigma \rho_\sigma(k). \tag{E.8}$$

In this form the magnetization can be incorporated into the integral expression (E.6):

$$\begin{aligned} g(T,h) &= \frac{1}{2}\sum_\sigma \int_{-\pi}^{+\pi} \frac{\mathrm{d}k}{2\pi} \Big\{ \rho_\sigma(k) \sin k + k_B T \Big[\rho_\sigma(k) \ln \rho_\sigma(k) + \big(1-\rho_\sigma(k)\big) \ln \big(1-\rho_\sigma(k)\big) \Big] \\ &\quad - h\sigma \rho_\sigma(k) \Big\}. \end{aligned} \tag{E.9}$$

The variation for any spinon density ρ_σ is

$$\delta g(T,h) = \frac{1}{2} \sum_\sigma \int_{-\pi}^{+\pi} \frac{\mathrm{d}k}{2\pi} \Big(\sin k - h\sigma + k_B T \ln \frac{\rho_\sigma(k)}{1-\rho_\sigma(k)} \Big) \delta\rho_\sigma(k). \tag{E.10}$$

It vanishes independently of T and h only if the term in brackets vanishes identically. Solving for ρ_σ immediately leads to

$$\rho_\sigma(k) = \frac{1}{1 + \mathrm{e}^{\beta(\sin k - h\sigma)}}. \tag{E.11}$$

F Neutron Optics

Main results of the presented work are the asymptotics and finite-size formulas for the dynamic spin structure factor $S_{+-}(q,\omega)_0$ (see Sec. 3.4). Spin structure factors are, as many dynamic properties of condensed matter in general, open to experimental analysis. Many experiments have been performed in the field of neutron optics where the scattering of neutrons is used to analyze dynamic properties of condensed matter states. Therefore we shall include a small chapter on neutron scattering here.
The main point of this technique is that the neutrons interact with the magnetic moments of nuclei and unpaired electrons, but not with the tight-bound inner electrons. They are therefore sensitive to magnetic effects only and can easily penetrate the crystal. The energy is usually chosen to be around 25meV. These slow thermal neutrons ($\sim$ 300K) have a wavelength of some Ångström which is the same order of magnitude as the distance between the interaction loci. At the same moment, the energy is of the same order as typical excitation energies so that scattering processes are favored. Thus the interior of the material can be accessed. Having the purely magnetic interaction of the XX or Haldane-Shastry Hamiltonian in mind, neutrons are the ideal objects for scattering experiments. In the following we will briefly scetch the theory of neutron scattering. The presentation follows the textbooks [48, 49].
The scheme of the usual experiments is as follows: A beam of well-controlled neutrons with all the same energy and momentum is scatterd by a crystal (the target). All around the target detectors measure the energy and (vectorial) momentum of the outgoing neutrons. The theory can now help in two different ways: (i) *a priori* it helps to design the appropriate experiments by predictions of the energies where the interaction with the crystal is large and (ii) *a posteriori* the measured scattering angles and exchange of energy and momentum can be compared with the theory.
The key of any theoretical analysis is the partial differential cross-section which gives the respond of the target to the incident neutrons. It depends in a trivial way on the neutron's dynamical properties and in a complicated way on the inner structure of the crystal. But this dependence can be separated and put into the so-called *structure factor*. In the framework of the Born approximation [50] the partial cross-section is given explicitely by [48]

$$\frac{\mathrm{d}^2\sigma}{\mathrm{d}\Omega \mathrm{d}E'} = \frac{|\vec{k}'|}{|\vec{k}|}\Big(\frac{m}{2\pi}\Big)^2 \sum_{\sigma,\lambda} p_\lambda p_\sigma \sum_{\sigma',\lambda'} \Big|\langle \sigma'\lambda'| \int \mathrm{d}\vec{r}\, \mathrm{e}^{-\mathrm{i}\vec{k}'\cdot\vec{r}}\, V(\vec{r})\, \mathrm{e}^{+\mathrm{i}\vec{k}\cdot\vec{r}} |\sigma\lambda\rangle\Big|^2 \delta(\hbar\omega + E_\lambda - E_{\lambda'}). \qquad \text{(F.1)}$$

The notation is chosen such that the wave numbers of the neutron are $\vec{k}$ before the scattering and $\vec{k}'$ afterwards. Accordingly, the neutron's energy before and after the scattering is E and E', respectively. We then define the exchange of wave number and energy by $\vec{q} = \vec{k} - \vec{k}'$ and

$$\hbar\omega = \frac{\hbar^2}{2m}(\vec{k}^2 - \vec{k}'^2) = E - E'. \qquad \text{(F.2)}$$

This notations are consistent with the previous given formulas (3.61) and (3.62) if the periodicity of the Brillouin zone and the cosine dispersion relation of the spinons is taken into account and the units of energy and momentum are chosen such that $\hbar = 1$. Of course, m is the mass of the neutron. The initial and final state of the target are $|\lambda\rangle$ and $|\lambda'\rangle$ with energies E_λ and E'_λ. Similarily, the neutron spin states are named $|\sigma\rangle$ and $|\sigma'\rangle$. Hence the summation over $\lambda, \sigma, \lambda', \sigma'$. The potential V is the effective interaction potential for nuclear and magnetic scattering. The Born approximation means that the initial and final state of the neutron are assumed to be plane waves. The Dirac δ-function in (F.2) expresses the conservation of energy. The initial states of the target and the initial spin states of the neutron are distributed with the probabilities p_λ and p_σ.
Our studies in Sec. 3.4 are restricted to transitions from the ground state. Thus p_λ would be one for the ground state and zero for any other state. This restriction can be incorporated into the experiment

by cooling the target sufficiently close to the absolute zero. The potential will normally depend on the loci of the scattering centers,

$$V(\vec{r}) = \sum_j V_j(\vec{r} - \vec{R}_j). \tag{F.3}$$

We insert this expression in (F.1) and write

$$\bar{V}_j(\vec{q}) = \int \mathrm{d}\vec{r}\, V_j(\vec{r}) \mathrm{e}^{\mathrm{i}\vec{q}\cdot\vec{r}} \tag{F.4}$$

for the Fourier transform. Additionally, we now neglect the possible spin polarization of the neutron to obtain

$$\frac{\mathrm{d}^2\sigma}{\mathrm{d}\Omega \mathrm{d}E'} = \frac{|\vec{k}'|}{|\vec{k}|}\Big(\frac{m}{2\pi}\Big)^2 \sum_{\lambda,\lambda'} p_\lambda \big|\langle\lambda'|\sum_j \bar{V}_j(\vec{q})|\lambda\rangle\big|^2 \delta(\hbar\omega + E_\lambda - E_{\lambda'}). \tag{F.5}$$

Next we make use of the integral definition of the δ-distribution and write the cross-section as

$$\frac{\mathrm{d}^2\sigma}{\mathrm{d}\Omega \mathrm{d}E'} = \frac{|\vec{k}'|}{|\vec{k}|}\Big(\frac{m}{2\pi}\Big)^2 \int_{-\infty}^{+\infty} \mathrm{d}t\ \mathrm{e}^{\mathrm{i}t(\hbar\omega + E_\lambda - E_{\lambda'})} \sum_{j,j'}\sum_{\lambda,\lambda'} p_\lambda\ \langle\lambda'|\bar{V}_j(\vec{q})|\lambda\rangle^\dagger\ \langle\lambda'|\bar{V}_{j'}(\vec{q})|\lambda\rangle. \tag{F.6}$$

Adopting the usual definition

$$\langle O_1 O_2\rangle = \sum_\lambda p_\lambda \langle\lambda|O_1 O_2|\lambda\rangle = \sum_{\lambda,\lambda'} p_\lambda \langle\lambda|O_1|\lambda'\rangle\,\langle\lambda'|O_2|\lambda'\rangle \tag{F.7}$$

of the correlation function of two arbitrary operators O_1 and O_2 we express (F.5) via the Heisenberg operators

$$V(\vec{q},t) = \exp\Big(\frac{\mathrm{i}}{\hbar}tH\Big)\bar{V}(\vec{q})\exp\Big(-\frac{\mathrm{i}}{\hbar}tH\Big) \tag{F.8}$$

where H is the Hamilton operator of the target system,

$$\frac{\mathrm{d}^2\sigma}{\mathrm{d}\Omega \mathrm{d}E'} = \frac{|\vec{k}'|}{|\vec{k}|}\Big(\frac{m}{2\pi}\Big)^2 \frac{1}{\hbar}\int_{-\infty}^{+\infty} \mathrm{d}t\ \mathrm{e}^{\mathrm{i}\omega t} \sum_{j,j'} \langle V_j^\dagger(\vec{q},0) V_{j'}(\vec{q},t)\rangle. \tag{F.9}$$

Since both operators are the same (at different times) for Hermitian potentials, the correlation function is the *autocorrelation function* of the potential.
The important point of this formula is the factorization into dynamical properties of the neutrons and interaction with the target. The dynamical part is completely controlled by experiment and the properties of the target material are in the end all summed up to a single function

$$S(\vec{q},\omega) = \frac{1}{2\pi} = \int_{-\infty}^{+\infty} \mathrm{d}t\ \mathrm{e}^{\mathrm{i}\omega t} \sum_{j,j'} \langle V_j^\dagger(\vec{q},0) V_{j'}(\vec{q},t)\rangle. \tag{F.10}$$

which is called the *structure factor*. In the application on spin chains the potential operator $\bar{V}(\vec{q})$ is the spin fluctuation operator

$$S_q^\mu = \frac{1}{\sqrt{N}}\sum_{j=1}^{N} \mathrm{e}^{\mathrm{i}qj} S_j^\mu, \qquad \mu = x,y,z \tag{F.11}$$

where N is the chain length, $q = 2\pi l/N$, $l = 1, 2, \ldots, N$ the wave number and $S_j = \sigma_j/2$ the Pauli matrix divided by one half. In the notation used in Chaps. 2.4 and 3.4 the *dynamic spin structure factor* is defined to be

$$S_{\mu\mu}(q,\omega)_0 = 2\pi \sum_{\lambda'} \left|\langle 0|S_q^\mu|\lambda'\rangle\right|^2 \delta(\hbar\omega - \omega_{\lambda'}), \qquad \mu = z, +, - \tag{F.12}$$

for transitions from the ground state $|0\rangle$. This common notation was already used in the early textbook style article [51].

References

[1] Thales of Miletus. Thales lived from c. 624 to c. 545 BC and his original work did not survive. But according to Aristotle's text *De Anima* he believed the lodestone to house a soul.

[2] M. Planck. Über eine Verbesserung der Wienschen Spektralgleichung. *Verhandl. Dtsch. phys. Ges.* **2**, 202–204 (1900).

[3] A. Einstein. Über einen die Erzeugung und Verwandlung des Lichtes betreffenden heuristischen Gesichtspunkt. *Ann. Phys.* **17**, 132–148 (1905).

[4] N. Bohr. On the Spectrum of Hydrogen. *Fysisk Tidsskrift* **12**, 97 (1914). The work has been published in Danish.

[5] W. Gerlach and O. Stern. Der experimentelle Nachweis der Richtungsquantelung im Magnetfeld. *Z. Phys.* **9**, 349–351 (1922).

[6] G. E. Uhlenbeck and S. Goudsmit. Discovery of Spin. *Naturwiss.* **47**, 953 (1925).

[7] E. Schrödinger. Quantisierung als Eigenwertproblem I. *Ann. Phys.* **79**, 361–376 (1926). The work continues in three subsequent articles.

[8] W. Heisenberg. Über quantentheoretische Umdeutung kinematischer und mechanischer Beziehungen. *Z. Phys.* **33**, 879–893 (1925).

[9] M. Born, W. Heisenberg, and P. Jordan. Zur Quantenmechanik. II. *Z. Phys.* **35**, 557–615 (1926).

[10] W. Heisenberg. Zur Theorie des Ferromagnetismus. *Z. Phys.* **49**, 619 (1928).

[11] H. Bethe. Zur Theorie der Metalle. I. Eigenwerte und Eigenfunktionen der linearen Atomkette. *Z. Phys.* **71**, 205 (1931).

[12] F. D. M. Haldane. Exact Jastrow-Gutzwiller Resonating-Valence-Bond Ground State of the Spin-$\frac{1}{2}$ Antiferromagnetic Heisenberg Chain with $1/r^2$ Exchange. *Phys. Rev. Lett.* **60**, 635 (1988).

[13] B. S. Shastry. Exact Solution of an $S = \frac{1}{2}$ Heisenberg Antiferromagnetic Chain with Long-Ranged Interactions. *Phys. Rev. Lett.* **60**, 639 (1988).

[14] J. des Cloizeaux and M. Gaudin. Anisotropic Linear Magnetic Chain. *J. Math. Phys.* **7**, 1384 (1966).

[15] L. A. Takhtadzhan and L. D. Faddeev. The quantum method of the inverse problem and the Heisenberg XYZ model. *Usp. Mat. Nauk.* **34**(5), 13 (1979).

[16] N. Kitanine, J. M. Maillet, and V. Terras. Form factors of the XXZ Heisenberg spin-$\frac{1}{2}$ finite chain. *Nucl. Phys. B* **554**, 647 (1999).

[17] D. Biegel, M. Karbach, and G. Müller. Transition rates via Bethe ansatz for the spin-1/2 planar XXZ antiferromagnet. *J. Phys. A: Math. Gen* **36**, 5361 (2003).

[18] D. Biegel, M. Karbach, G. Müller, and K. Wiele. Spectrum and transition rates of the XX chain analyzed via Bethe ansatz. *Phys. Rev. B* **69**, 174404 (2004).

[19] W. Heitler and F. London. Wechselwirkung neutraler Atome und homöopolare Bindung nach der Quantenmechanik. *Z. Phys.* **44**, 455–472 (1927).

[20] W. Heitler. Störungsenergie und Austausch beim Mehrkörperproblem. *Z. Phys.* **46**, 47–72 (1927).

[21] L. D. Faddeev and L. A. Takhtadzhan. Spectrum and Scattering Excitations in the One-Dimensional Isotropic Heisenberg Model. *J. Soviet Math.* **24**, 241 (1984).

[22] P. P. Kulish and E. K. Sklyanin. Solutions of the Yang-Baxter Equation. *Zap. Nauchn. Sem. LOMI* **95**, 129 (1982).

[23] L. D. Faddeev. How Algebraic Bethe Ansatz works for integrable model. *hep-th/9605187* (1996).

[24] V. E. Korepin, N. M. Bogoliubov, and A. G. Izergin. "Quantum Inverse Scattering Method and Correlation Functions". Cambridge University Press, Cambridge (1993).

[25] F. H. L. Essler, H. Frahm, F. Göhmann, A. Klümper, and V. E. Korepin. "The One-Dimensional Hubbard Model". Cambridge University Press, Cambridge (2005).

[26] K. Fabricius and B. M. McCoy. Bethe's Equation is Incomplete for the XXZ Model at Roots of Unity. *J. Stat. Phys.* **103**, 647 (2001).

[27] K. Fabricius and B. M. McCoy. Completing Bethe's Equation at Roots of Unity. *J. Stat. Phys.* **104**, 573 (2001).

[28] L. D. Faddeev and L. A. Takhtadzhan. Spectrum and Scattering of Excitations in the One-Dimensional Isotropic Heisenberg Model. *J. Sov. Math.* **24**, 241 (1984).

[29] V. E. Korepin. Calculation of Norms of Bethe Wave Functions. *Commun. Math. Phys.* **86**, 391–418 (1982).

[30] N. A. Slavnov. Calculation of Scalar Products of Wave Functions and Form Factors of the Algebraic Bethe Ansatz. *Theor. Mat. Fiz.* **79**, 232 (1989).

[31] M. Karbach, G. Müller, A. H. Bougourzi, A. Fledderjohann, and K.-H. Mütter. Two-spinon dynamic structure factor of the one-dimensional $s = \frac{1}{2}$ Heisenberg antiferromagnet. *Phys. Rev. B* **55**, 12510 (1997).

[32] P. Jordan and E. Wigner. Über das Paulische Äquivalenzverbot. *Z. Phys.* **47**, 631 (1928).

[33] E. Lieb, T. Schultz, and D. Mattis. Two Soluble Models of an Antiferromagnetic Chain. *Ann. Phys.* **16** (1961).

[34] M. Arikawa, M. Karbach, G. Müller, and K. Wiele. Spinon excitations in the XX chain: spectra, transition rates, observability. *J. Phys. A: Math. Gen.* **39**, 10623 (2006).

[35] S. Katsura. Statistical Mechanics of the Anisotropic Linear Heisenberg Model. *Phys. Rev.* **127**(5), 1508 (1962).

[36] K. Huang. "Statistical Mechanics". John Wiley & Sons, New York (1987).

[37] L. D. Faddeev and L. A. Takhtadzhan. What is the Spin of a Spin Wave? *Phys. Lett.* **A85**, 375 (1981).

[38] F. D. M. Haldane. "Spinon Gas" Description of the $S = \frac{1}{2}$ Heisenberg Chain with Inverse-Quare exchange: Exact Spectrum and Thermodynamics. *Phys. Rev. Lett.* **66**, 1529 (1991).

[39] M. Karbach, G. Müller, and K. Wiele. Interaction and thermodynamics of spinons in the XX chain. *cond-mat/07103097* (2007).

[40] I. S. Gradshteyn and I.M. Rhyzhik. "Tables of Integrals, Series, and Products". Academic Press Inc., Orlando, Florida (1980).

[41] G. Müller, H. Thomas, H. Beck, and J.C. Bonner. Quantum spin dynamics of the antiferromagnetic linear chain in zero and nonzero magnetic field. *Phys. Rev. B* **24**, 1429–1467 (1981).

[42] F. D. M. Haldane. Physics of the Ideal Semion Gas: Spinons and Quantum Symmetries of the Integrable Haldane-Shastry Spin Chain. *Springer Series in Solid State Sciences* **118**, 3 (1994).

[43] J. C. Talstra. Integrability and Applications of the Exactly-Solvable Haldane-Shastry One-Dimensional Quantum Spin Chain. *cond-mat/9509178* (1995).

[44] B. M. McCoy, E. Baruch, and D. B. Abraham. Statistical Mechanics of the XY Model. IV. Time-Dependent Spin-Correlation Functions. *Phys. Rev. A* **4**, 2331 (1971).

[45] E. R. Hansen. "A Table of Series and Products". Prentice-Hall, Englewood Cliffs, NJ (1975).

[46] H. T. Davis. "The Summation of Series". The Pricipia Press of Trinity University, San Antonio, Texas (1962).

[47] M. Abramowitz and I. Stegun. "Pocketbook of Mathematical Functions". Dover Publications, New York (1984).

[48] S. W. Lovesey and T. Springer. "Dynamics of Solids and Liquids by Neutron Scattering". Springer-Verlag, Berlin (1977).

[49] E. Balcar and S. W. Lovesey. "Theory of Magnetic Neutron and Photon Scattering". Oxford Series on Neutron Scattering in Condensed Matter. Oxford University Press, Oxford (1989).

[50] A. Messiah. "Quantenmechanik". Walter de Gruyter, Berlin (1991).

[51] M. Karbach, K. Hu, and G. Müller. Introduction to the Bethe Ansatz III. *cond-mat/0008018* (2000).